COST COMPARISON OF EXISTING COATINGS FOR A HYPERVELOCITY TEST RAIL

THESIS

Mark A. Blomer, Ensign, USNR

AFIT/GAE/ENY/05-J01

DEPARTMENT OF THE AIR FORCE
AIR UNIVERSITY

AIR FORCE INSTITUTE OF TECHNOLOGY

Wright-Patterson Air Force Base, Ohio

AFIT/GAE/ENY/05-J01

COST COMPARISON OF EXISTING COATINGS FOR A HYPERVELOCITY TEST RAIL

THESIS

Presented to the Faculty

Department of Aeronautics and Astronautics

Graduate School of Engineering and Management

Air Force Institute of Technology

Air University

Air Education and Training Command

In Partial Fulfillment of the Requirements for the

Degree of Master of Science in Aeronautical Engineering

Mark A. Blomer, BS

Ensign, USNR

June 2005

AFIT/GAE/ENY/05-J01

COST COMPARISON OF EXISTING COATINGS FOR A HYPERVELOCITY TEST RAIL

Mark A. Blomer, BS

Ensign, USNR

Approved:

_____ */signed/*_____	*20050606*
Dr. Anthony N. Palazotto (Chair)	Date
_____ */signed/*_____	*20050606*
Dr. Theodore Nicholas (Member)	Date
*/signed/*_____	*20050606*
Dr. William P. Baker (Member)	Date

AFIT/GAE/ENY/05-J01

Abstract

This study compared the relative costs, to the Department of Defense, of two different coatings used to protect a high speed test rail. Each coating was compared to the case of an uncoated rail with test conditions that caused catastrophic failure just after the test sled reached its maximum velocity. The total cost was finalized on a per test basis in order to sum the costs of various expenditures that may only occur once every few tests.

To compare the protective properties of each coating, various coated and uncoated samples were tested via a cylinder specimen Taylor Impact Test. Each coating's protective properties, or coating effectiveness, were found by its radial deformation change at the impacted end of each cylinder relative to the uncoated cylinder. This deformation change, relative to the uncoated cylinder's deformation change, was the coating's effectiveness.

Taylor Test results were then analyzed using the CTH hydrocode. CTH is able to model Taylor Impact Tests. CTH was used to understand the internal workings and results of the Taylor Tests in more depth. Verification between CTH and experimental Taylor Tests was done using final values for length, diameter and undeformed length of the cylinder.

Acknowledgments

Table of Contents

List of Figures

List of Tables

Nomenclature

$	US dollars
D	diameter
D_0	initial diameter
D_1	final diameter
r	radius
L	length
L_0	initial length
L_1	final length
L_{UD}	undeformed length
t	time
V	volume
dV	differential volume
P	pressure
ρ	material density
F	force
m	mass
dv	differential velocity
dt or $\varDelta t$	differential time step
μ	Coulomb friction coefficient
I	impulse
v_o	initial velocity
v_1	final velocity
E	internal energy
E_0	initial internal energy source
E_1	final internal energy source
$W_{0 \rightarrow 1}$	work done on a system in going from state 0 to state 1
A	area
C_P	specific heat
dA	differential area
x	position
dx	differential length
σ	stress
σ_Y	yield stress
E_m	modulus of elasticity
G	shear modulus
ν	Poisson's ratio
U	wave velocity
u	particle velocity
L	length
ε	strain
$\dot{\varepsilon}$	strain rate

$\dot{\varepsilon}_p$ plastic strain rate

IE_0, IE_1 initial and final internal energy

KE_0, KE_1 initial and final kinetic energy

$f(\ )$ function of

Johnson-Cook Constitutive Equation

A, B, C, m, n Johnson-Cook coefficients

T^* homologous temperature

T_{room} room temperature

T_{melt} material melting temperature

T absolute temperature

Equation of State

$[\sigma]$ stress tensor

$[\sigma_d]$ deviatoric stress tensor

$[\sigma_h]$ hydrostatic stress tensor

Γ Grüneisen Parameter

C_1, C_2, C_3 Mie-Grüneisen coefficient

**COST COMPARISON OF EXISTING COATINGS FOR A HYPERVELOCITY
TEST RAIL**

Chapter 1 – Introduction

In recent years, the United States Air Force (USAF) has spent considerable

money and effort investigating methods to improve the understanding of very high

velocity impact testing. The Air Force utilizes a sophisticated test facility located at

Holloman Air Force Base (AFB) in New Mexico to perform the majority of the advanced

tests. The main system consists of a narrow gauge rail system approximately ten miles

long, which is used to guide a rocket sled, see Figure 1, at extremely high velocities. In

April 2003, the Holloman High Speed Test Track (HHSTT) achieved a world record

velocity of 2884.9 m/s. The 846th Test Squadron, which operates the HHSTT, is working

to increase the maximum velocity to 10,000 ft/s or approximately 3 km/s. [1]

Figure 1: Rocket Sled at HHSTT

In achieving such high velocities the steel on steel interface between the sled and

the rail create a phenomenon known as gouging shown in Figure 2 [2]. Gouges are

typically 15.0 cm long by about .6 cm deep. Given enough velocity these gouges lead to catastrophic failure of the test. To mitigate this problem various coatings have been applied to the rail. This form of protection was studied by Szmerekovsky. He found that adding a coating did decrease the occurrence and severity of gouging. Currently the two most effective coatings have been epoxy adhesive (epoxy) and iron oxide (oxide).
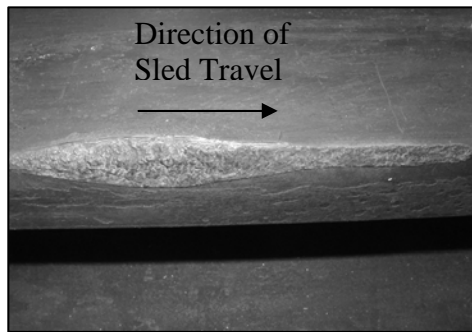
Figure 2: Gouged Rail Section

The primary objective of this thesis is to compare the total cost, to the Department of Defense (DOD), per test for each an uncoated, epoxy coated, and oxide coated rail. Neither facility at the Air Force Institute of Technology (AFIT) nor at the Air Force Research Lab (AFRL) was able to simulate actual HHSTT conditions during gouging. A scaled model was created by Rickerd [1] which is able to scale the situation down to one which could be simulated by AFRL in the Taylor Impact Test (Taylor Test). With this test, a baseline comparison of the results for an uncoated, impacted cylinder was compared to that of a cylinder coated with each oxide and epoxy. One result of this test was the increase in radial deformation of each coated sample over the uncoated sample. This became known as the coating's effectiveness. Besides material cost, this effectiveness is the most significant factor in comparing the total cost per test of each coating, the primary objective of this thesis.

Chapter 2 - Background and Theory

2.1 Equations of State

It is common when solving dynamic mechanics problems to break down stress and strain into two components, the hydrostatic or volumetric stress or strain and the deviatoric stress or strain,

$$[\sigma] = [\sigma_h] + [\sigma_d] \qquad (1)$$

Where $[\sigma]$ is the stress tensor, $[\sigma_h]$ is the hydrostatic stress tensor, and $[\sigma_d]$ is the deviatoric stress tensor. The hydrostatic stress is often called the volumetric stress because it is the stress that develops a volume change for a given parallelepiped of material, while the deviatoric stress is associated with a shape change. In impact problems, these two varieties of stress are handled via two separate relationships. The first of these relationships, the deviatoric stress, will be discussed in the next section on constitutive equations. The second relationship deals with the hydrostatic stress, and is called the equation of state. The two are taken separately because it has been found that hydrostatic stress is virtually independent of strength and plasticity, while deviatoric stress is only slightly dependent upon pressure. [3]

Additionally, equations of state are needed to model how pressure, density, and energy relate when compressibility effects and irreversible processes such as shock waves are included in the problem. [4]

The equation of state of a material describes the relationship between pressure, specific volume, and internal energy, and can be shown in a general form by

$$E = E(P,V)$$
(2)

Where E is the internal energy, P is the pressure, and V is the specific volume. An alternative form, often used in computer codes is shown below. [1]

$$P = P(\rho, E).$$
(3)

The Mie-Grüneisen equation of state, utilized in the epoxy coating, is a simple equation of state that is very good for modeling high-pressure shock related events [5]. The Mie-Grüneisen equation of state is based upon statistical mechanics, using the energy of individual atoms to arrive at thermodynamic equations. The Hugoniot pressure is used as a baseline in the Mie-Grüneisen equation of state and is given by,

$$P_H = C_1\mu + C_2\mu^2 + C_3\mu^3$$
(4)

Where P_H is the Hugoniot pressure, the C_i's are constants, and μ is

$$\mu = \frac{\rho}{\rho_o} - 1.$$
(5)

The *C* parameters in the equation for the Hugoniot pressure are only for a case where density increases. If density decreases, C_2 and C_3 are zero. The pressure is then calculated with

$$P = P_H\left(1 - \frac{\Gamma\mu}{2}\right) + \Gamma\rho(E - E_o) \qquad (6)$$

Where *E* is the internal energy per unit mass, E_o is the internal energy per unit mass at ambient conditions, and Γ is a constant called the Grüneisen parameter. The Grüneisen parameter is assumed to be independent of temperature and only a function of specific volume, and is represented below. [1]

$$\Gamma = V\left(\frac{\partial P}{\partial E}\right)_v . \qquad (7)$$

The equation of state used in this investigation for every other material except epoxy isn't actually an equation at all. It is in fact simply a table that correlates pressure, energy, and density at various states. In CTH, this equation of state is called the SESAME model. Two major advantages of a tabular equation of state are that there is no need to calculate equation of state variables, as they are simply part of a table, and that by using a tabular equation of state the exact physical state is used as opposed to an assumed state, i.e. a quadratic form as in the Mie-Grüneisen equation of state. This can be very important if the pressures applied are high enough that a material will change state from solid to liquid or liquid to gas. [1]

2.2 Constitutive Equations

The relationship between stress and strain in continuum mechanics codes is dictated by a constitutive equation. In most finite element codes, stress is assumed to be quasi-static, which means that the loading is applied so slowly that there aren't any dynamic loading effects. In quasi-static cases, the most common constitutive equation used is the classic Hooke's Law equation,

$$\sigma = f(\varepsilon, E_m) \qquad (8)$$

Where σ is the stress, ε is the strain, and E_m is the modulus of elasticity. In many situations however, it is inappropriate to assume that stress is applied quasi-statically, because of this, Hooke's Law will only be used in cases where the stress is below the yield stress of the material. In cases where the applied stress is greater than the yield stress, it is necessary to account for dynamic loading effects. The most common way to account for dynamics in a continuum mechanics problem is to include strain rate as a variable in the constitutive equation. In general this becomes,

$$\sigma = f\left(\varepsilon, \dot{\varepsilon}, E_m\right) \qquad (9)$$

Where $\dot{\varepsilon}$ is the strain rate applied. In some cases, constitutive equations will also be a function of internal energy and damage. [2]

CTH, a finite element program hydrocode developed by Sandia National Laboratories, provides numerous constitutive equations with which stress-strain behavior

6

can be modeled. Most of these equations will be of little use in this impact study,

because constitutive equations tend to be very problem specific. Constitutive equations

exist for metals, ceramics, concrete, and soil amongst others. [1]

One of the most basic, yet still valuable, constitutive models available in CTH is

the Johnson-Cook Strength Model. This model presents the Von Mises flow stress as

$$\sigma = (A + B\varepsilon^n)(1 + C \ln \dot{\varepsilon}_p)(1 - T^{*m})$$
(10)

where σ is the von Mises flow stress, ε is the equivalent plastic strain, $\dot{\varepsilon}_p$ is the plastic

strain rate normalized by a strain rate of $1.0\mathrm{s}^{-1}$, T^* is defined below, and *A, B, C, m,* and

n are the Johnson-Cook coefficients for the given material. The Johnson-Cook

viscoplastic material model accounts for temperature via the homologous temperature, T^*

which is given as

$$T^* = \frac{T - T_{room}}{T_{melt} - T_{room}}$$
(11)

Where *T* is the absolute temperature, T_{room} is the ambient temperature, and T_{melt}, is the

melting temperature of the material. [3]

There are two minor disadvantages to the Johnson-Cook model. The first is that it

presents strain rate sensitivity as being independent of temperature, which in general is

not the case. However, by keeping strain, strain rate, and temperature uncoupled, it

becomes relatively straightforward to determine the Johnson-Cook coefficients from a

few simple experiments at various temperatures and strain rates. The second

disadvantage of the Johnson-Cook model is that it is strictly a mathematical curve-fit of

experimental data, and is therefore not built upon a base of physics. [1]

Chapter 3 – Methodology

3.1 Johnson-Cook Coefficient Verification

The accurate prediction of the performance of impacting and explosively formed metals requires high strain rate descriptions of material behavior. One such description is the Johnson-Cook model, which was originally developed for the accurate prediction of explosively formed metal penetrators. The Johnson-Cook model was specifically developed from a set of well-defined laboratory data, including low and high strain rate tests as well as elevated temperature tests. [6]

Extensive work was done to solve for the 1080 steel coefficients via Johnson-Cook coefficients. Hopkinson Bar Tests [7] were conducted for various high strain-rate variable temperature results. The results of the 1080 steel J-C material property investigation (Kennan coefficients) were used in CTH simulation.

To verify these coefficients, they were input, along with the other required properties of 1080 steel, shown in Table 7, into Cook's *2-Dimensional Axisymmetric Lagrangian Solver for Taylor Cylinder Impact with Johnson-Cook Constitutive Model* (Taylor-Cook Solver). Cook created this program for rapid verification of model coefficients for various materials. The advantage of the Taylor-Cook Solver was its speed and ease of simulation. Its speed of iteration was contrasted by the fact that it uses a Lagrangian solver.

A Lagrangian solver does not allow for material to pass into or out of a cell within the mesh. This leads to errors in specimens with large deformations. For use with a Taylor test at velocities low enough to prevent major fractures, cracks and buckling this method is adequate. In addition to the use at lower velocity impacts, the Taylor-Cook Solver's purpose was only to verify coefficients with a visual inspection of deformation to a cylinder. The method of a Lagrangian method versus an Eulerian method is covered in detail in reference [1].

3.2 CTH Solution Method

CTH was developed by Sandia National Laboratories to "model multidimensional, multi-material, large deformation, strong shock wave physics" [8] problems. CTH originated as a hydrodynamic, Computational Fluid Dynamics (CFD), code. It has since been advanced to include tension and shear strength, giving it the capability to model strength of material problems. A complete verification that CTH can accurately model a Taylor Test can be found in references [1,2]. The details applicable to modeling the specific Taylor Tests are discussed below.

One defining characteristic of CTH when compared to a typical hydrocode is that CTH models the ability of materials to support a deviatoric, or shearing, stress. In hypervelocity gouging problems, one of the main deformation causing processes is believed to be the slipper sliding along the rail in a shearing action on the rail. CTH provides two options to model a sliding interface between two materials. [1]

The default method for material interfaces in CTH is to assign a very high strength value to mixed material cells. This means that any two materials in contact were treated as if they were welded or bonded together [9]. This was the simplest of the three boundary conditions considered and was effective in obtaining results when varying other input parameters because it did not require an extremely fine mesh size.

An alternative algorithm is the slide line, as it is called in CTH. It takes a different approach to handling material interfaces. It sets the deviatoric stress at the material boundary to zero. The material boundary is defined as any number of cells in

the CTH mesh where the two materials are both present, a mixed cell. This option

effectively turns the projectile's surface into a liquid, since it is unable to support any

frictional forces. [9].

This method tended to yield erroneous results especially in higher impact

velocities, due to large thermodynamic errors. Most simulations at these higher velocities

could not be completed. Intuitively the coating and target do not create a frictionless

interface so no results from this boundary condition will be shown.

The third method used was the boundary layer, seen as "blint" in the CTH input

file in Appendix 2. Using this algorithm required a designation of a hard, the target, and

a soft, the coating, material. The soft material was then deformed and otherwise affected

according to the third CTH input, the coefficient of friction. A very fine mesh was

required in order to keep the mixed material cells isolated to the coating and the target. If

a coarse mesh was used then the frictional boundary layer would spread to the 1080 and

large errors would result. This was visualized by seeing 1080 being ejected from the

impact area as a liquid shown below.
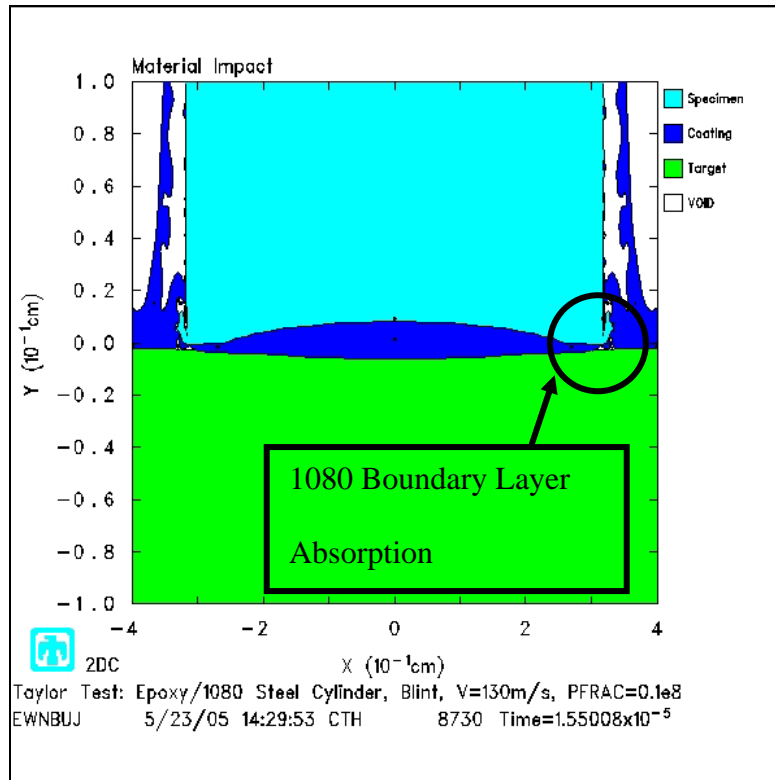
Figure 3: Epoxy, 130 m/s, Boundary Layer,

Lowered Fracture Pressure, 15 μs

The mesh was also limited from being too fine because errors would be created as a result of over meshing the simulation. CTH was based on macro-level mechanics. Meshing finer cells than 0.002 cm square was considered going beyond the scope of macro-mechanics. [9]

3.3 Coating Cost Method

To make a decision of what coating to use, cost versus benefit must be shown. Information was gathered from the HHSTT regarding material and labor costs as well as time lost for various processes. In addition, a few underlying assumptions were made in order to associate experimental and numerical data with actual test conditions. From ref [10] it was assumed that radial deformation in the Taylor Test is proportional to coating effectiveness at the HHSTT.

"For the last five years, the rail alignment criteria have been consistent and different from the previous 45 [years]. The numbers [requested] apply from 2000-present"[11]. Some information regarding catastrophic failure (failure) was taken from the Patriot tests [10] which date back to 1997 because no failure has been reported since 2000.

Some definitions need to be stated. Chipping was any damage to the coatings that requires reapplication in addition to the regularly scheduled coating removal and re-application. Failure was defined as the catastrophic destruction of the test vehicle, the payload, test sled, and generally about 2 sections, 78 feet, of rail that all have to be replaced. The payload included everything that was being tested.

In addition to the radial deformation assumption, a few others were made. What would be chipping to a coated rail was considered minor to an uncoated rail and was neglected. Usually the uncoated section was the initial, low speed, section of the test track and rail sections are rarely damaged. Also, the cost per test difference between

sand and water blasting was negligible (around $500 per test). If the entire track was

uncoated, there was no chipping repair cost, only total failure replacement cost. Finally,

failure replacement cost was the dollar amount it takes the Department of Defense to

replace all components lost in a failure.

Chapter 4 – Analysis and Results

4.1 Taylor Test

From reference [1] it was shown that the Taylor Impact Test can accurately model the gouging problem seen at the HHSTT when properly scaled. However, for the objective of this thesis the full gouge does not need to be initiated. Instead a 1080 cylinder projectile was shot at a VascoMax 300 target at various speeds. This deformed the projectile rather than penetrating the target. Only right angle impact was considered. Four different types of cylinder specimens were tested, VascoMax 300, 1080 Steel, iron oxide coated 1080, and epoxy coated 1080. These can be seen in Figure 4.

Figure 4: Taylor Test Samples (6cm long by 0.6 cm diameter), Right to left, VM300, 1080 Steel, Oxide 1080, and Epoxy 1080

These specimens were all shot at a VascoMax 300 target in the experimental set- up shown in Figure 5 and Figure 6.

16
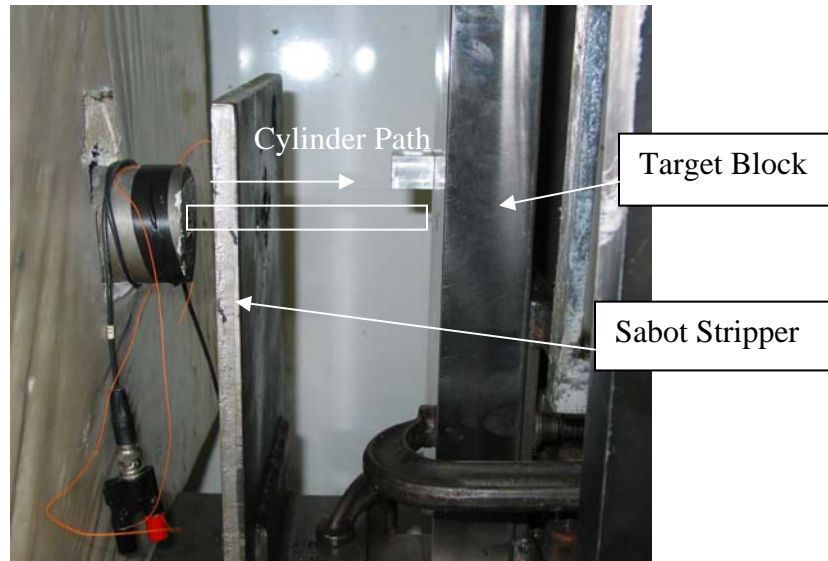
Figure 5: Taylor Test Target Impact

The target block was held in place using multiple C-clamps. The actual cylinders being shot were pushed through the pipe by a plastic sabot because their diameter was too small for the pipe. This sabot was stripped off by the steel plate just after exiting the pipe. The pressure source and valves for launching the cylinder are shown below:
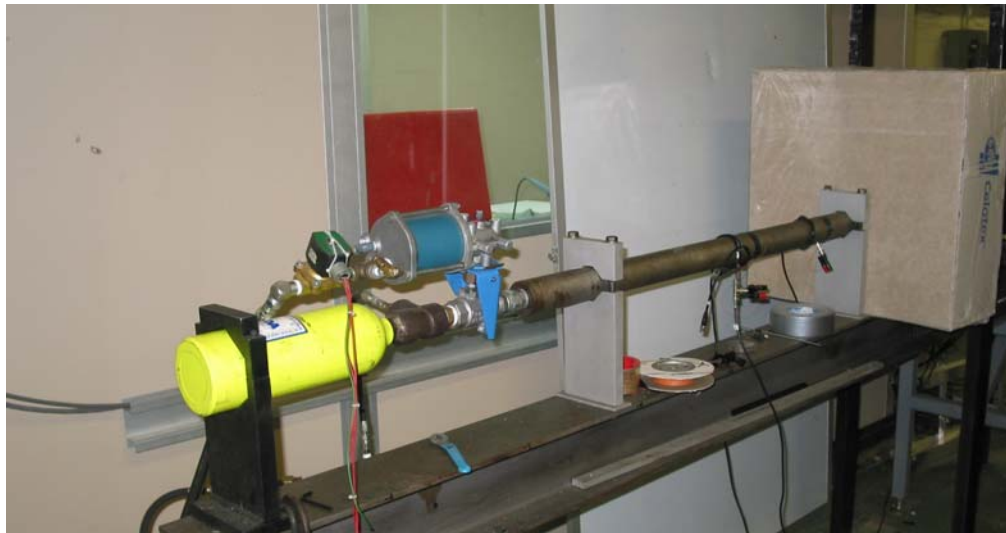
Figure 6: Taylor Test Pressure Source and Valves

Four tests from the Taylor tests were used to model in CTH. Their results are shown in Table 1. Only 1080 steel was coated in order to simulate the rail being coated.

Table 1: Experimental Taylor Test Results

| | | Impact | | Cylinder Length | | |
| | | V_{impact} | Duration | L_o | L_1 | εL |
Coating	Test #	(m/s)	(μs)	(cm)	(cm)	(%)
Iron Oxide	I2	130.00	63.00	6.019	5.790	3.805
Epoxy	E5	128.00	63.00	6.048	5.737	5.142
Iron Oxide	I4	243.00	63.00	3.028	2.625	13.309
Epoxy	E4	243.00	63.00	3.510	2.631	25.043

Table 2: Experimental Taylor Test Results (Cont'd)

| | | Undeformed Length | | Nose Diameter | | | |
| | | L_{UD} | L_{UD} / L_o | D_o | D_1 | εD | D_1 / D_o |
Coating	Test #	(cm)	(%)	(cm)	(cm)	(%)	(%)
Iron Oxide	I2	3.74	0.62	0.630	0.665	5.556	1.06
Epoxy	E5	3.94	0.65	0.625	0.690	10.400	1.10
Iron Oxide	I4	1.07	0.35	0.593	0.970	63.575	1.64
Epoxy	E4	1.42	0.41	0.597	1.020	70.854	1.71

Where L_1 is the final length, L_0 is the initial length, D_0 is the initial diameter of the deformed end, D_1 is the final diameter of the deformed end and εL and εD are given by the definition for strain from ref [12].

$$\varepsilon D = \frac{D_1 - D_0}{D_o} \tag{12}$$

$$\varepsilon L = \frac{L_1 - L_0}{L_o} \tag{13}$$

The velocity of the projectile was determined from the high speed camera shown in Figure 7.
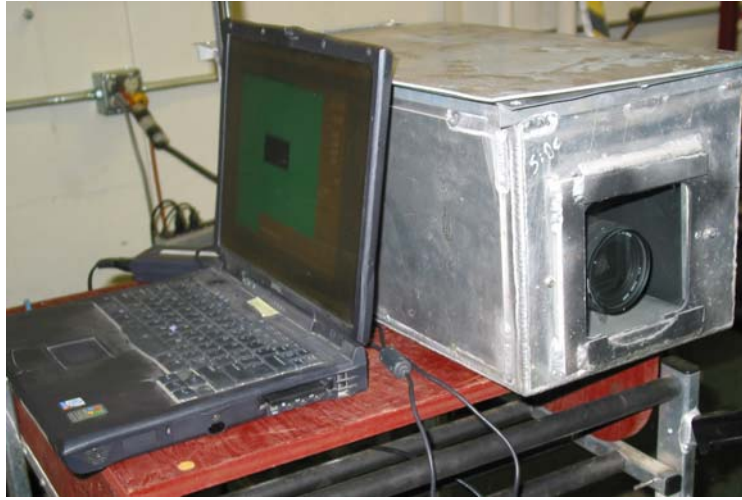
Figure 7: High Speed Camera

The film strip from test E4 shown in Figure 8 was used to approximate impact velocity and contact time with the target for test E4. All film strips showed a typical contact time of the projectile with the target of 63 μs for the four experimental Taylor Test Results simulated in CTH. Each frame had a Δt of 21 μs so all contact times are 63 +/- 10.5 μs.
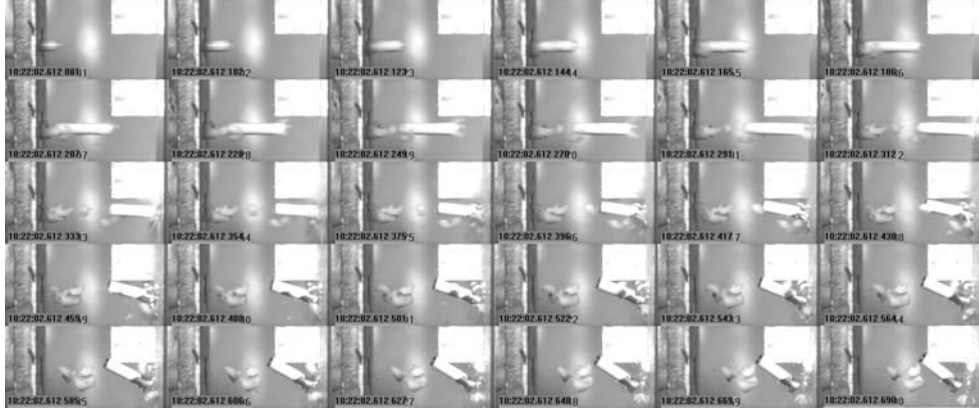
Figure 8: Taylor Shot E4, Epoxy Coated 1080 Steel, V=243m/s

No tests with impact velocities greater that 243 m/s were used because massive fracturing or buckling occurred in the projectile and final dimensions would be impossible to find. The results of the experimental Taylor Tests were then compared to simulations in CTH. To simplify the simulation inputs one cylinder was modeled at 6 cm long by 0.6 cm in diameter. Samples in the experimental results varied slightly in dimensions. Taylor test results were equated to expected CTH results via strain, shown below.

$$D_{CTH} = \frac{D_{0,CTH}}{\varepsilon D_{Taylor} + 1} \qquad (14)$$

$$L_{CTH} = \frac{L_{0,CTH}}{\varepsilon L_{Taylor} + 1} \qquad (15)$$

$$L_{UD,CTH} = \frac{L_{UD}}{L_{0,Taylor}} \cdot L_{0,CTH} \qquad (16)$$

Where $L_{o, CTH}$ is 6 cm and $D_{o, CTH}$ is 0.6 cm for the CTH simulations.

The expected values in CTH were:

20

Table 3: Expected Values for CTH Output

Coating	Test #	V_{impact} (m/s)	Expected for CTH		
			L_1 (cm)	L_{UD} (cm)	D_1 (cm)
Iron Oxide	I2	130.00	5.78	3.73	0.635
Epoxy	E5	130.00	5.71	3.91	0.670
Iron Oxide	I4	243.00	5.30	2.12	1.647
Epoxy	E4	243.00	4.80	2.43	2.059

From the results of the experimental Taylor Test, Figure 9, we see that relative to the uncoated cylinder, oxide deforms radially to a greater degree and that epoxy deforms even more so than oxide.

Taylor Impact Specimen Diameter Change v. Impact Velocity
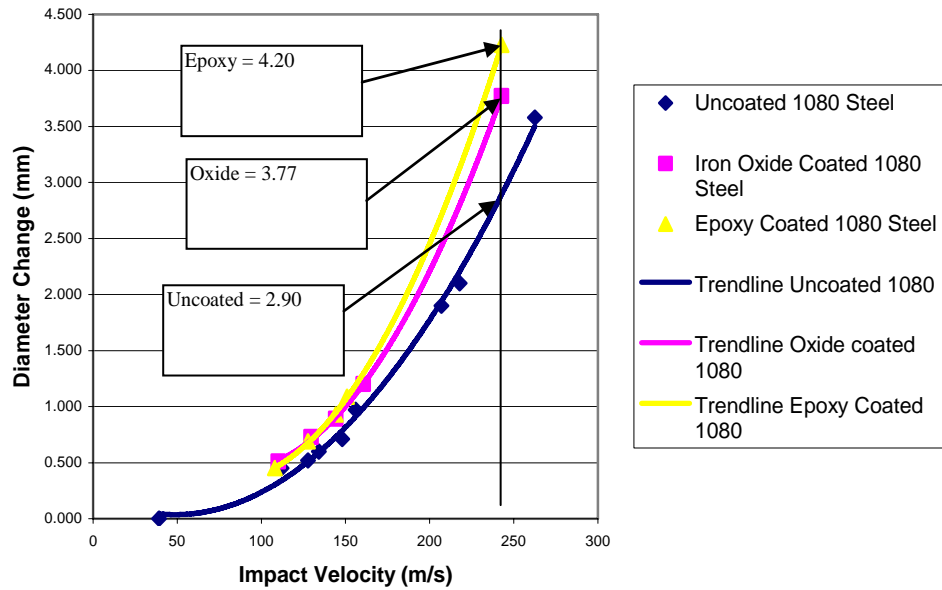
Figure 9: Diameter Deformation Ratio vs. Impact Velocity for Epoxy, Oxide, and Uncoated

From Figure 9 we found the coating effectiveness. Where:

$$\% \, effetive_{coating} = \frac{(D_1 - D_0)_{coated}}{(D_1 - D_0)_{uncoated}} \qquad (17)$$

For example:

$$23\% = 1 - \frac{2.90}{9.7 - 5.93} \qquad \textit{(18), Oxide Coating Effectiveness}$$

$$31\% = 1 - \frac{2.9}{10.2 - 5.97} \qquad \textit{(19), Epoxy Coating Effectiveness}$$

As seen in the experimental Taylor Test results. Coating effectiveness was taken at the maximum usable velocity found in experimental results which was 243 m/s. The percent increase of oxide over uncoated 1080 steel was 23% and epoxy over uncoated 1080 is 31%. That means for epoxy impacting at 243 m/s the radial deformation percent it will function 31% better than an uncoated specimen.

4.2 CTH Simulations

The validity of using CTH to model the Taylor test was verified by Rickerd, ref [1], who created the initial CTH model of a Taylor test. It has since been modified to more closely show what's happening in a Taylor test. Some of the primary choices in modeling the Taylor Test were the mesh size, material properties, material constitutive equations, and the interaction between different materials or boundary conditions.

4.2.1 Mesh Sizing

Properly sizing the mesh was an iterative process that is crucial to obtaining accurate results from any finite element code. Material sizes and locations can be seen in Figure 10. The coating around the 1080 cylinder was 0.02 cm thick [11]. The 1080 cylinder is 6 cm long by 0.6 cm in diameter. The target was 6 cm in height and 12 cm in diameter. The mesh was refined around the area of interest to cells 0.002 cm square in Figure 11. This maped the coating with 10 cells though the thickness of the coating on the face of the cylinder and along the circumference in the area of impact.

Figure 10: CTH Material Set-Up

Figure 11: CTH Mesh for Taylor Impact Test

This particular mesh was chosen to give a maximum refinement around the area of impact. In that area each cell was 0.002 cm square. A minimum cell size was needed to get a maximum number of cells within the coating, a thickness of 0.02 cm on the face and side of the cylinder. Any smaller mesh size than this and the materials no longer behaved as a continuum. Mechanic behavior became typical of the micro level rather than the macro level [10]. Cells in the out-lying regions were coarser to limit the total number of cells in the mesh and thus decrease the simulation time.

In order to obtain deformation results that were as accurate as possible, tracer points were inserted through out the material. When assessing the undeformed length in CTH, any radial deformation for the profile tracer points within 0.01 cm of the original radius was considered undeformed. The locations for all the tracer points are shown in Figure 12. The view shows only one half of the cylinder as it is modeled in CTH.
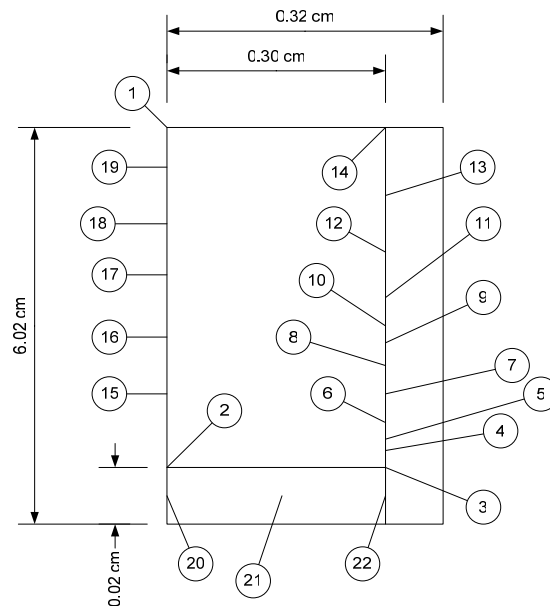
Figure 12: Tracer Point Locations

25

The tabulated x and y locations of each tracer point are:

Table 4: Tracer point Locations via X, Y Coordinates

Tracer Pt	X	Y	Tracer Pt	X	Y
1	0.000	6.020	12	0.299	4.020
2	0.000	0.021	13	0.299	5.020
3	0.299	0.021	14	0.299	6.020
4	0.299	0.270	15	0.000	1.020
5	0.299	0.520	16	0.000	2.020
6	0.299	0.770	17	0.000	3.020
7	0.299	1.020	18	0.000	4.020
8	0.299	1.520	19	0.000	5.020
9	0.299	2.020	20	0.000	0.010
10	0.299	2.520	21	0.150	0.010
11	0.299	3.020	22	0.300	0.010

Locations of tracer points on the edges of the 1080 cylinder were placed inward from the edge by 0.001 cm to avoid mixed material cells distorting results as much as possible while maintaining as much accuracy as possible.

Results from the tracer points for final length, shown in Appendix 3, represent the top and bottom centerline positions of the cylinder, tracer points 1 & 2. Radial deformation velocity is shown for points 3 and 4. Some simulations showed a very large radial velocity for point 3 when it was absorbed into the boundary layer. That information was disregarded. In this case tracer point 4 was used to estimate radial deformation velocity. The radial velocity was used to determine if extreme deformation

velocities existed and would neglect the application of a Coulomb friction coefficient [13]. As seen in reference [14] effective friction coefficient was decreased as velocity is increased to a large degree. For all tests, the maximum radial velocity was 80 m/s. This does not diminish the validity of the Coulomb friction coefficient.

4.2.2 Material Properties

Previously the 1080 steel cylinder was modeled by a Johnson-Cook constitutive equation for iron because there was no 1080 steel material in CTH. This proved to be inaccurate. Proper coefficients for a Johnson-Cook model were taken from ref [15]. The Kennan coefficients are shown below.

Table 5: Coefficients for Johnson-Cool Model of 1080 Steel

Constant	Value
A	0.525×10^9 Pa
B	3.59×10^9 Pa
C	0.029
m	0.674
n	0.6677
t	0.01581885

Available material properties for the two coatings, epoxy and oxide, were limited. From observations of experimental results it was assumed that each coating experienced very little yielding and that a model in which the coating fractured immediately upon yielding would be accurate. With this assumption the only material properties needed were Poisson's ratio and yield pressure.

27

The respective values for each coating, taken from the Szmerekovsky model ref [2], are

shown in below.

Table 6: Material Properties for Coatings

	Epoxy	Iron Oxide	
σ_Y	1.50E+08	2.00E+09	Dyne / cc
ν	0.46	0.25	
μ	0.30	0.60	

Where σ_Y is the yield strength, ν is Poisson's Ratio, and μ is the coefficient of friction.

Friction coefficient properties were estimated using ref [16]. Modulus of elasticity is

assumed based on user inputted yield strength and an assumed strain offset of 0.2% [9].

The Kennan coefficients were initially verified using the "2D Axisymmetric

Lagrangian Solver for Taylor Cylinder Impact with Johnson-Cook Constitutive Model"

solver (Taylor Cook Solver).
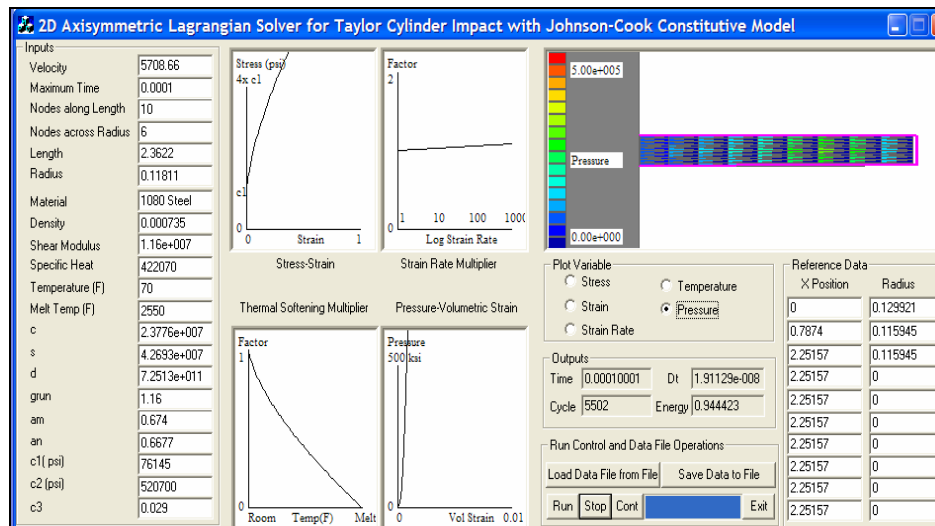
Figure 13: Taylor Cook Solver Screen Shot,

28

The advantage of the Taylor Cook Solver was its speed and ease of simulation. That was sided with the fact that it used a Lagrangian solver. A Lagrangian solver does not allow for material to pass into or out of a cell within the mesh. This leads to errors in specimens with large deformations. This method is adequate for use with a Taylor test at velocities low enough to prevent fractures, cracks and buckling, less than 243 m/s. For informative purposes, the method of a Lagrangian solver versus an Eulerian solver is covered in detail in references [1, 2].

The Kennan coefficients were verified using the conditions of test S9 in Appendix 1.

Table 7: Taylor-Cook Solver Inputs for Test S9

1080 Steel			
V_{impact}	5708.66 in / sec	c1	7.61E+04 psi
t	1.00E-04 sec	c2	5.21E+05 psi
L	2.3622 in	c3	2.90E-02
r	0.11811 in	am	6.74E-01
ρ	7.35E-04 slug / in^3	an	6.68E-01
G	1.16E+07 psi	c	2.38E+07
Cp	4.22E+05 in*lbf / slug F	s	4.27E+07
T	7.00E+01 F	d	7.25E+07
T_{melt}	2.55E+03 F	grun	1.16

Their description can be found in Table 8.

Table 8: Johnson-Cook coefficient Relations and Descriptions

Johnson-Cook Coefficients in Solver		
Display	Report	Description
c1	A	Yield Strength (psi)
c2	B	Work Hardening Extent (psi)
c3	C	Strain Rate Effect
am	m	Thermal Softening Shape
an	n	Work hardening Shape

Values for equations of state properties; c, s, d, and grun were taken from Cook's 4340

steel example included with the Taylor-Cook Solver. This was assumed to be accurate

because in a Taylor Test the material was not changing state. If extreme velocities are

used and a phase change occurs then large deformations are likely to exist and the

Lagrangian solution method breaks down and causes its own errors. The result is shown

in Figure 14. The purple line is the expected result.
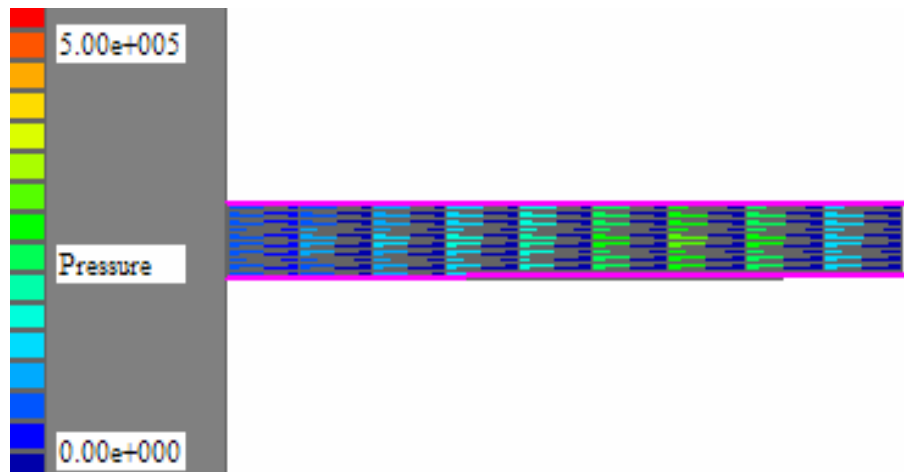
Figure 14: Taylor-Cook Solver Test S9, Result Final Deformation

Unfortunately a scaling or zoom option was not available within the Taylor-Cook Solver and a coarse visual estimation tends to be the best option. The image has been enlarged as much as practical for analysis. It can be seen that the deformation is within acceptable limits of experimental results. The purple line represents the deformation seen in the experimental lab test. The Kennan coefficients have been verified and are ready to be inputted into the CTH model for simulating a coated specimen Taylor Test.

4.2.3 Material Interfaces

There were three choices for boundary conditions between the coating and the target. These choices were no slip, frictional boundary layer, and a slide line condition. Each of these were considered and simulated. A thorough investigation of each condition is available in ref [13]. The slide line was the least useful in modeling attempts and allowed too much deformation and thermodynamic errors within the CTH result.

The profile for the no slip choice of boundary condition was similar to experimental results as can be seen when comparing Figure 15 and Figure 16 for an epoxy coated 1080 steel test at 130 m/s with an epoxy fracture pressure of 1.5e8 Dynes/cc as well as in Figure 17 and Figure 18 for a 243 m/s test.

The Comparison is shown below:

Figure 15: Taylor Test E5, Epoxy, 130 m/s

Figure 16: CTH, Epoxy, 130 m/s, No Slip

The light blue is the 1080 steel, the dark blue is the epoxy coating and the green is the

VascoMax 300 target.

For the 130 m/s case it was difficult to see any difference between the CTH result

and the actual result. We can see the fracturing of the epoxy coating up to about one

third of the final length or about 1 – 2 cm. The CTH result did not show this fracturing.

This inconsistency between CTH and actual results can be remedied by lowering the

fracture pressure of the coating. Lower fracture pressure, and its associate lower yield

strength, results will be shown later in this section.

The 243 m/s case illustrates a difference between the profile of the experimental

result and CTH's result. The actual profile was more representative of a bell shape curve

in the first 1 to 2 cm of the impact face. In the CTH model the deformation was

distributed along a much larger piece of the cylinder length.
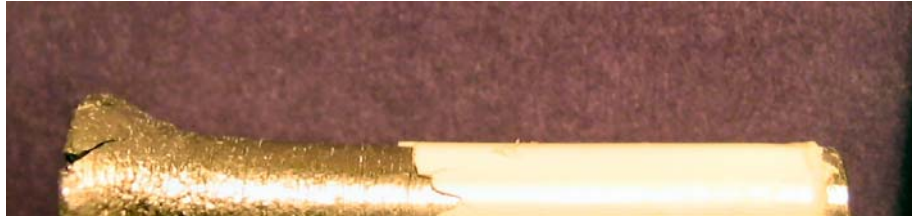
Figure 17: Taylor Test E4, Epoxy, 243 m/s

Figure 18: CTH, Epoxy, 243 m/s, No Slip

The bell type curve is clearly visible on the actual specimen. The coating has fractured on the actual specimen up to about half of the original length. The CTH has no fracture in the coating. This leads to the idea that a more complete modeling of the coating material properties is needed. With a relatively low impact velocity the "No slip" condition yields good results for final dimensions but not for deformations profile.

These results for final diameter, length and undeformed length are:

Table 9: CTH Expected Results vs. CTH No Slip Results and % Error

Coating	Test #	V_{impact}	Expected for CTH L_1	L_{UD}	D_1	CTH Results - No Slip L_1	L_{UD}	D_1	% Error L_1	L_{UD}	D_1
		(m/s)	(cm)	(cm)	(cm)	(cm)	(cm)	(cm)	%	%	%
Iron Oxide	I2	130.00	5.78	3.73	0.635	5.66	3.21	0.632	2.08%	13.90%	0.52%
Epoxy	E5	130.00	5.71	3.91	0.670	5.68	3.50	0.650	0.47%	10.46%	2.93%
Iron Oxide	I4	243.00	5.30	2.12	1.647	5.15	1.29	0.692	2.74%	39.16%	57.99%
Epoxy	E4	243.00	4.80	2.43	2.059	5.19	1.28	0.706	8.16%	47.38%	65.71%

For a model more representative of actual conditions, the frictional boundary layer condition was used. The fracture pressure is held at 1.5e8 Dynes/cc. Results are shown only for epoxy coating but they are representative of both epoxy and oxide. Both coatings began to fracture at the same fracture pressure despite different Poisson's Ratios. This is because of the limited material constitutive equations.

Frictional values were taken from [16] and averaged to be about 0.3 for epoxy and 0.6 for oxide. Using a frictional boundary layer did require a very fine mesh and a relatively long time to simulate. It also made determining the final diameter a bit challenging when 1080 would get absorbed into the boundary layer. We will see this cause more problems later as the fracture pressure of the coating is lowered to match experimental results and impact speed increases. If the mesh was too coarse, the tracer

point measuring final diameter, tracer point 3 would actually be taken in by the boundary later and the material it represented would be converted into a fluid like substance. A visual inspection and comparison with the next tracer point along the profile, tracer point 4, still yielded good results. The frictional boundary layer result for 130 m/s is shown in Figure 20.

Figure 19: Taylor Test E5, Epoxy, 130 m/s
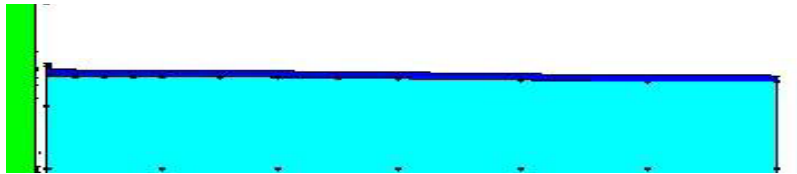
Figure 20: CTH, Epoxy, 130 m/s, Frictional Boundary Layer

Again it appears that CTH deformations results are very close to experimental results at 130 m/s.

Let's take a look at the 243 m/s case.
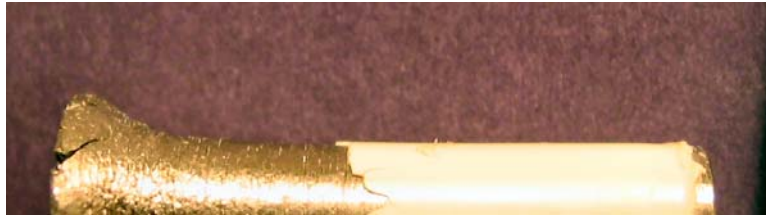
Figure 21: Taylor Test, E4, 243 m/s

Figure 22: CTH, Epoxy, 243 m/s, Frictional Boundary Layer

The figures above again show that the profile is not characteristic of the actual Taylor test

for 243 m/s impact velocity. The numerical results for final diameter, length and

undeformed length compared to expected values for all four tests are shown in Table 10.

We see a good agreement between CTH and experimental results in the 130 m/s case.

Table 10: CTH Expected Values vs. CTH Boundary Layer Results and % Error

Coating	Test #	V_{impact} (m/s)	Expected for CTH L_1 (cm)	L_{UD} (cm)	D_1 (cm)	CTH Results - Boundary Layer L_1 (cm)	L_{UD} (cm)	D_1 (cm)	% Error L_1 %	L_{UD} %	D_1 %
Iron Oxide	I2	130.00	5.78	3.73	0.635	5.67	3.42	0.636	1.99%	8.27%	0.11%
Epoxy	E5	130.00	5.71	3.91	0.670	5.69	3.50	0.634	0.38%	10.46%	5.32%
Iron Oxide	I4	243.00	5.30	2.12	1.647	5.13	1.33	0.830	3.12%	37.27%	49.61%
Epoxy	E4	243.00	4.80	2.43	2.059	5.20	1.56	0.824	8.45%	35.87%	59.97%

The fracture pressure mentioned earlier in this section was then lowered to 1.0e7 Dynes/cc, which was lower than minimum published values found in ref [16]. This value was arrived at after some iteration within CTH. The results of a 130 m/s impact can be seen in Figure 24 for a no slip boundary interface.

They can be compared to the previous CTH simulation using values from ref [2] and the actual results.

Figure 23: Taylor Test E5, Epoxy, 130 m/s

Figure 24: CTH, Epoxy, 130m/s, No Slip, Lowered Fracture Pressure

Figure 25: CTH, Epoxy, 243 m/s,

This Comparison shows fracturing consistent with experimental results.

Deformation results for the 1080 cylinder with coating fracture are shown in Table 11.

Table 11: CTH Results, Epoxy, No Slip, Coating Fracture

No Slip - Coating Fracture		Expected for CTH				CTH Results			% Error		
		V_{impact}	L_1	L_{UD}	D_1	L_1	L_{UD}	D_1	L_1	L_{UD}	D_1
Coating	Test #	(m/s)	(cm)	(cm)	(cm)	(cm)	(cm)	(cm)	%	%	%
Epoxy	E5	130.00	5.71	3.91	0.670	5.68	3.50	0.634	0.47%	10.46%	5.32%
Epoxy (Coating Fracture)	E5	130.00	5.71	3.91	0.670	5.68	3.50	0.640	0.41%	10.46%	4.43%
Epoxy	E4	243.00	4.80	2.43	2.059	5.20	1.28	0.706	8.37%	47.38%	65.71%
Epoxy (Coating Fracture)	E5	243.00	4.80	2.43	2.059	5.20	1.44	0.710	8.33%	40.74%	65.52%

We see that values for both final length and undeformed length are the same. The final diameter was slightly larger even for this relatively low velocity. It also appears that the profile in the sample with a fractured coating was slightly closer to the experimental result. The next step was to run a simulation at 243 m/s. This yielded results a little bit closer to experimental results. No major improvements were seen other than that the coating fractures as it does by observation from the lab. Undeformed length and final diameter are still in large error.

Trying to run a simulation with a lower fracture pressure and a frictional boundary layer was where the simulation ran into some trouble. Massive amounts of thermodynamic errors resulted, over 5,000,000 within the first 30 µs. These errors, usually existing in the form of a negative absolute temperature for a single cell, were present in most other simulations but not to such a degree, usually less than 100,000. A closer looks need to be taken at the material interface of the coating and target.

In Figure 26 we see the epoxy coated 1080 impacting at 130 m/s. It has a boundary layer established. We see at the edges of the cylinder that the 1080 is being sucked into the boundary layer created by the input file. Some 1080 material is being jetted out of the contact area as if it were a liquid. Unfortunately, the 1080 is mixing with the coating and target boundary layer and no amount of refining the mesh prevented this.
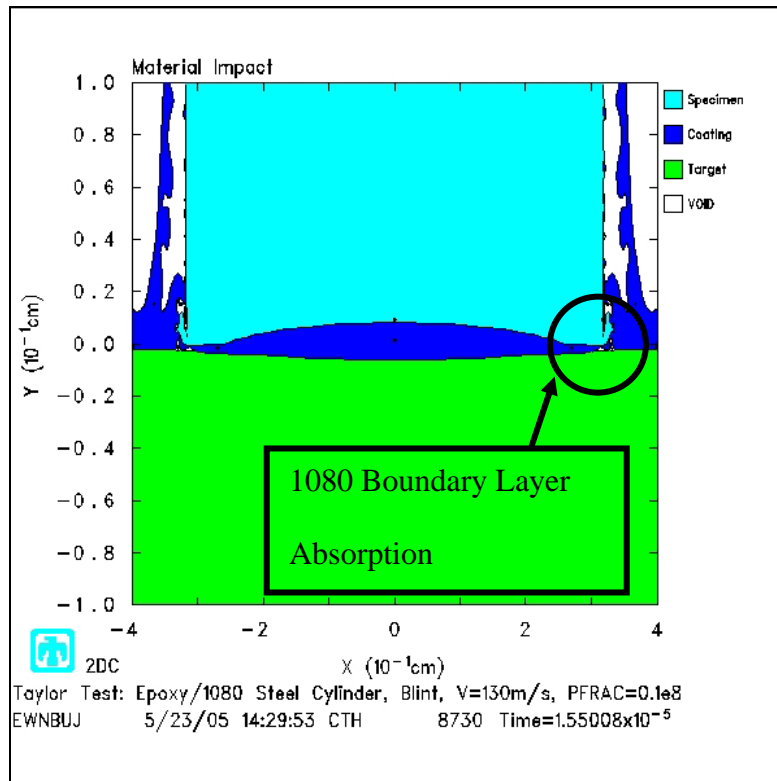
Figure 26: Epoxy, 130 m/s, Boundary Layer, Lowered Fracture Pressure, 15 µs

This is typical of both coatings and is seen to a greater degree when impact velocity is increased. A simulation was attempted at 243 m/s but it created too many thermodynamic errors too quickly and would not complete.

In the experimental Taylor Test the samples would bounce off the target block after about 63 μs of contact. Material interfaces in CTH did not allow this. In coated simulations the projectile appeared to bounce off the target after about 63 μs, just as in experimental results. What actually happened was the coating between the projectile and target fractured as seen in Figure 27.
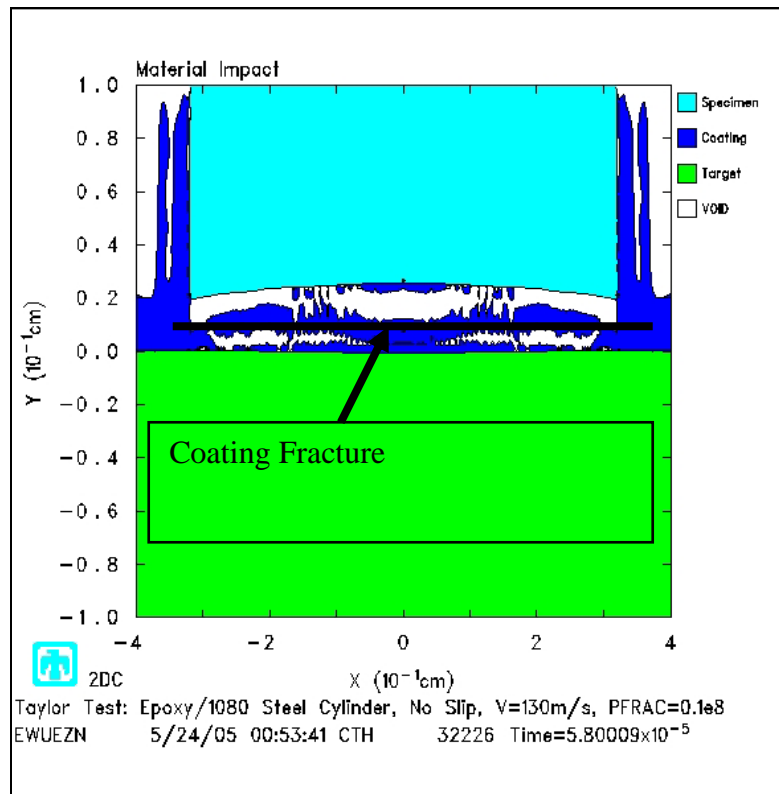
Figure 27: Epoxy, 130 m/s, No Slip,
Lowered Fracture Pressure, 58 μs

Temperature and pressure of the coating were of great interest. Comparing results from both the no slip and frictional boundary layer conditions it was found that they were nearly the same for a given impact velocity, with the exception of the cylinder edge when 1080 became entangled in the frictional boundary layer.

We see in Figure 28 the temperature distribution right before errors overtake the simulation. Notice the large temperatures at the cylinder edge.
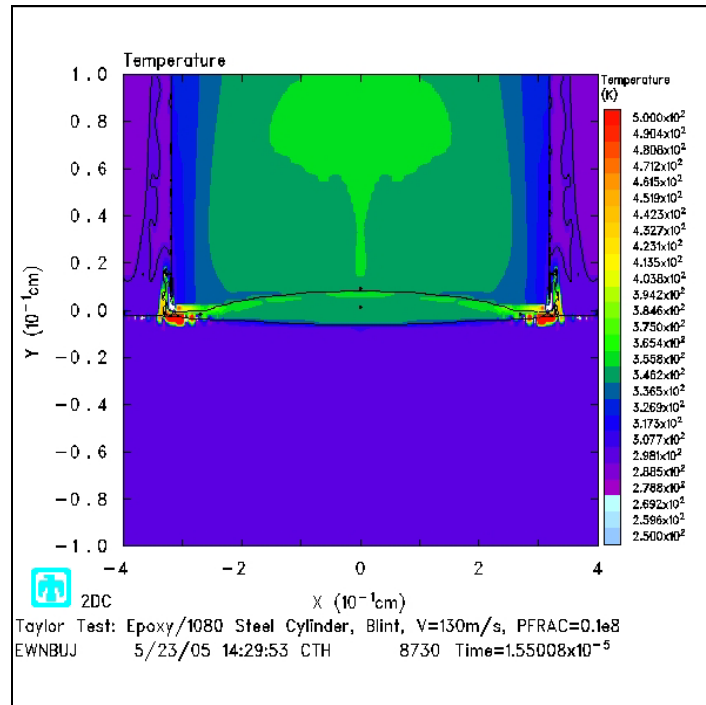
Figure 28: Temperature Epoxy, v=130 m/s, Boundary Layer, Reduced Fracture Pressure

Comparing the two different boundary conditions we see an agreement of increased temperature at the cylinder edge. It must also be noted that there is very little temperature increase in the coating on the circumference of the cylinder in both cases. It appears the only coating of value is that directly between the 1080 and the VM300.
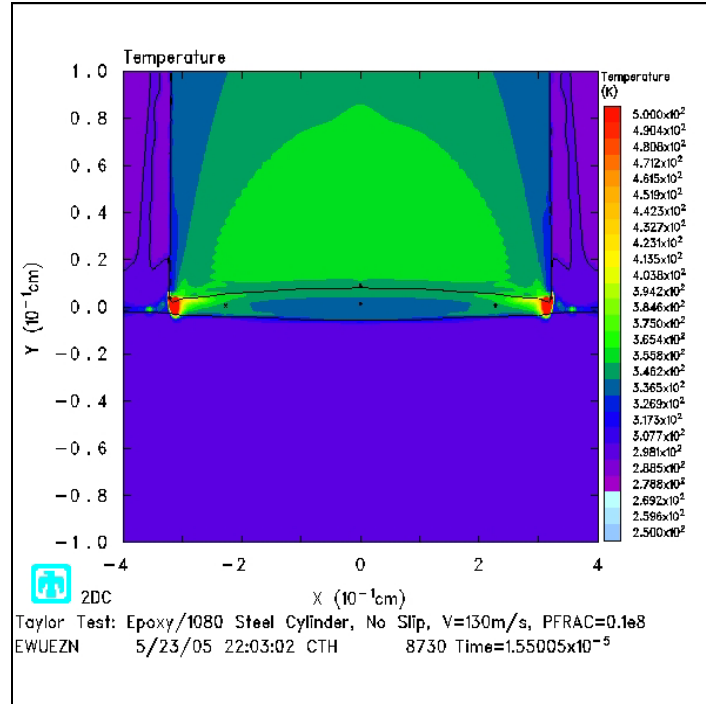
Figure 29: Temperature Epoxy, v=130 m/s, No Slip, Reduced Fracture Pressure

Temperature, and as we will see shortly pressure, are not distributed along the coating on the circumference of the cylinder.

Pressure was distributed between the face of the cylinder and the target. However, it was highest in the center rather than the edges of the projectile. Figure 30 shows a very high pressure of about 300 GPa at the center of the coating.
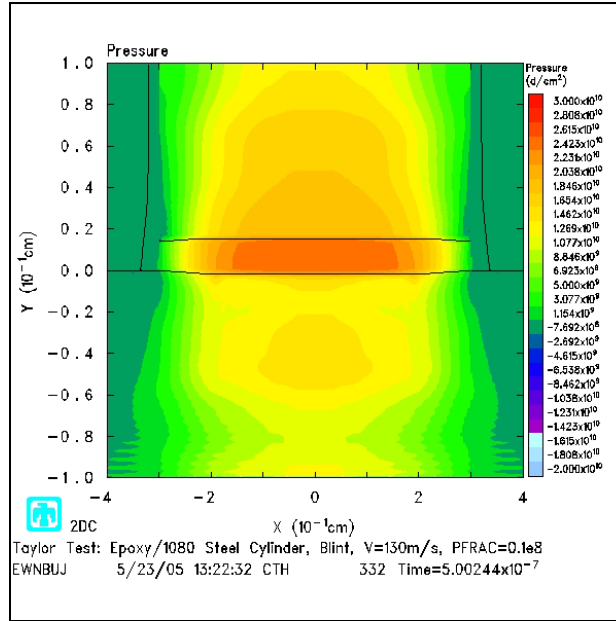
Figure 30: Pressure Epoxy, v=130 m/s, Boundary Layer, Reduced Fracture Pressure

Pressure was at a maximum immediately after impact at 5 µs. Its intensity was reduced

quickly as shown in Figure 31 by 15 µs to about 150 GPa, roughly half of its maximum

value.
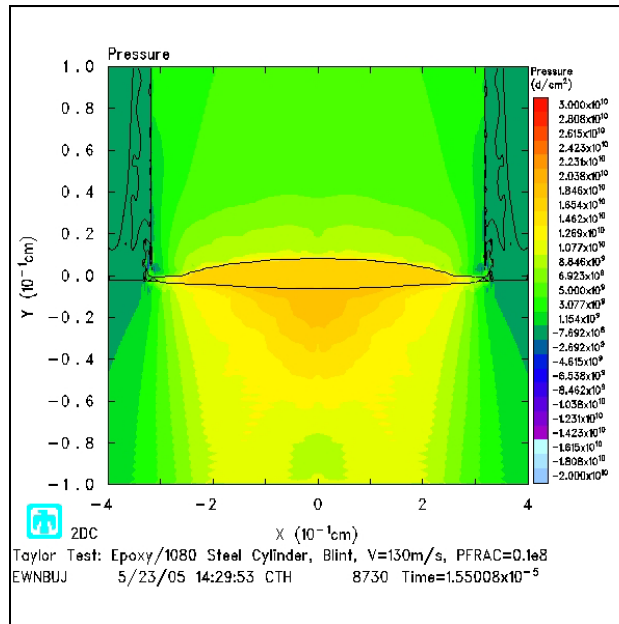
Figure 31: Pressure Epoxy, v=130 m/s, Boundary Layer, Reduced Fracture Pressure

Comparing the two boundary conditions from Figure 30 and Figure 31 to a no slip boundary interface in Figure 32 and Figure 33 we see little effect of boundary condition on the pressure distribution.
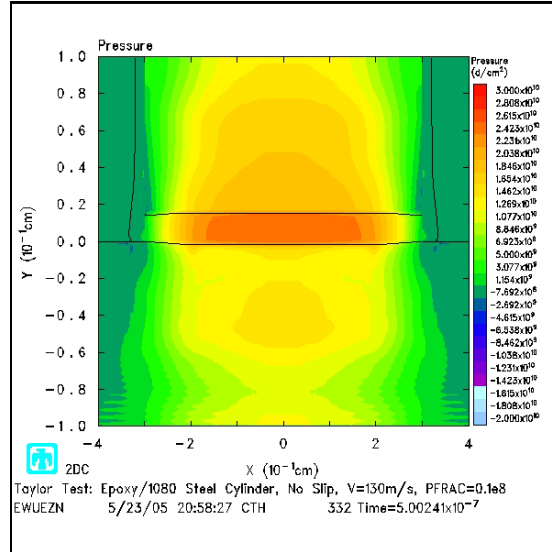
Figure 32: Pressure Epoxy, v=130 m/s, No Slip, Reduced Fracture Pressure
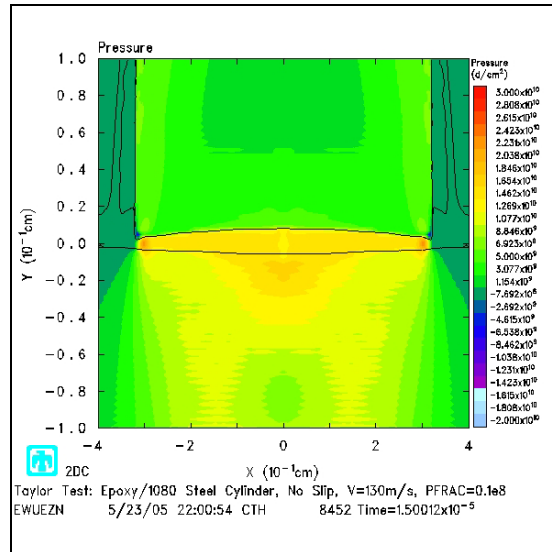
Figure 33: Pressure Epoxy, v=130 m/s, No Slip, Reduced Fracture Pressure

Results shown in Figure 32 and Figure 33 for a no slip condition are in agreement with those shown for the frictional boundary layer. A more complete collection of tracer point plots and material deformation can be found in Appendix 3 and Appendix 4 .

Some insight has been gained into the internal workings of pressure and temperature distribution during a Taylor Impact Test. Simulations at slower speeds are in good agreement with experimental results. Using the experimental results we found in the Taylor test, verified by CTH, a way to compare the effectiveness of each coating has been established. This coating effectiveness was then incorporated into a cost comparison.

4.3 Cost Comparison

Now that we have a way to compare the effectiveness of a coating we need to integrate that into a cost analysis. Shown in Figure 34, ref [10], are the results of a test run where catastrophic failure occurred just after the point of maximum velocity.
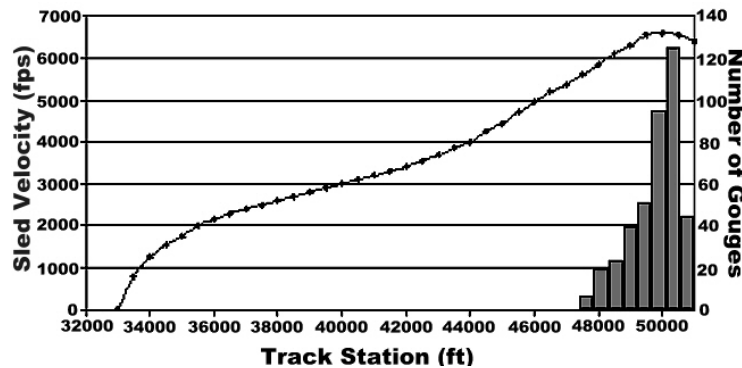
Figure 34: Actual HHSTT Results, Uncoated Test with Catastrophic Failure

It shows the location of gouges and velocity as a function of track position in feet. We see that virtually all gouging occurs in the high speed section at the end of the track. This information will be used in assessing the average cost per test seen by the DOD. It is this cost that is to be minimized. Key inputs for the cost per test were the amount of the rail that is to be coated and that coating's effectiveness factor, shown below.

Table 12: Initial Inputs for Cost Comparison

Initial Information				
Portion Coated	17600	17600	17600	ft / coating
Coating Effectiveness Factor	0.00%	23.00%	31.00%	reduced failure

47

Information was gathered from Holloman AFB, via Dr. Hooser (Hooser) [17] and Mr. John Furlow (Furlow) [11], regarding test set-up and material and labor costs. The comparison converted a wide array of inputs into a final cost per test for epoxy and oxide coatings. The base line case for cost comparison was a completely uncoated 10 mile long track in a test profile with approximately 175 feet of rail worth of chipping which catastrophically fails once every 12 test just as it reaches maximum velocity in the last portion of the rail. This was representative of Figure 34. Gouges are 6 in long on average and thus 350 total gouges are assumed. Some general information and assumptions common to all sections includes:

Table 13: Information Common to All Coatings and Areas of Cost

Workday	8.00	hr / day
1 section of rail	39.00	ft
Width of Coated Rail	9.50	in =
Track Length	52800.00	ft
Avg. Coating Thickness	0.02	cm
Uncoated test fails Once every	12	Tests
Cost of Rail	$1,000.00	per section
Replace	2	rail sections / failure

The cost comparison of coating the rail for a test has been broken down into three sections: a new rail coating, chipping repair/maintenance, and failure replacement costs. Tests were run once per month and there were no environmental clean up costs. The complete breakdown of each equation and results for each coating from total cost per test to the user inputs can be found in this section and Appendix 5.

All tables showing a breakdown of each cost are for 17,600 ft of uncoated, oxide and epoxy coated rail as seen in Table 13 with a $1,000,000 payload replacement cost. Total cost tables are just that, the total cost per test and are labeled for their respective coating distribution.

4.3.1   Initial Coating

A new rail coating, initial coating, refers to the cost of coating a clean rail. The initial coating is done after the rail is aligned. Rail alignment is included in the rail replacement cost. The actual coating is done with a machine built in-house at the test facility. This machine coats the rail with a thickness between 0.015 – 0.025 cm (~ 6 mils) at a speed of about 5 mph. The rails are coated in this fashion when a new rail is installed and after a sand or water blasting every four test runs. The cost break down for initial coating is shown in Table 14.

The process to find the cost per test of a coating application is the same for both coatings. We see below how we go from initial inputs to the initial coating result.

$$\frac{\$New\_Coat}{Test} = \frac{\$coat, initial}{ft, rail} \, x \, \frac{ft, rail}{coat} \, x \, \frac{1, coat}{\# tests} \qquad (20)$$

$$\frac{\$coat, initial}{ft, rail} = \frac{\$coat, initial}{1000\, ft, rail} \, x \, \frac{1}{1000\, ft} \qquad (21)$$

$$\frac{\$coat, initial}{1000\,ft, rail} = \frac{\$coat, initial}{gal} \, x \, \frac{\# gal}{1000\,ft} + \frac{\$Thinner}{gal} \, x \, \frac{\# gal}{1000\,ft} + \frac{Initial\_coat\_time}{1000\,ft} \, x \, \frac{\$Initial\_coat}{hr} \qquad (22)$$

$$\frac{Initial\_coat\_time}{1000\,ft} = \frac{hr, prep}{1000\,ft} + \frac{hr, Apply}{1000\,ft} + \frac{hr, Cleanup}{1000\,ft} \qquad (23)$$

The results of initial coating cost are shown in Table 14.

Table 14: Cost per Foot of Rail to Apply an Initial Coating to a Clean Rail

New Rail Coating	Uncoated	Iron Oxide	Epoxy	Units
Coating Application Cost	$0.00	$0.87	$2.03	per ft of rail

For the initial coating, it costs over twice as much to use epoxy as it does for the oxide, per foot of rail.

4.3.2 Chipping Maintenance

Chipping is defined as any damage to the coating requiring repair of the coating short of catastrophic failure and the rail is re-used. Virtually every time a test is run, 90% of test runs, some chipping occurs. It is assumed here that chipping occurs every test run. Chipping in a completely uncoated track will be considered under section 4.3.3 Failure only. In a completely or partially uncoated track chipping in the uncoated section is considered negligible because the uncoated sections will be in the areas of low velocity.

If both coatings are used in a test run then it is assumed that the chipping is distributed between the coatings in proportion to the amount of each coating that is used.

50

The total number of chips to be distributed to each coating is reduced by the effectiveness factor of the coating used. If the last section is coated with epoxy then the epoxy effectiveness factor is used for the total number of chips in both coatings. Otherwise the oxide effectiveness factor is used. An uncoated track is the baseline case and no effectiveness factor is used or needed.

The unit conversions for initial inputs to be converted to a cost of chipping per test are shown below.

$$\frac{\$Chipping}{Test} = \frac{\$Sand\_Treatment}{ft,rail} x \frac{ft,chips}{test} x \frac{ft,coating\_type}{ft,Total\_Coating} \tag{24}$$

$$\frac{\$Sand\_Treatment}{ft,rail} = \frac{\$Sand\_Blast}{ft,rail} + \frac{\$coating}{ft,rail} \tag{25}$$

$$\frac{\$Sand\_Blast}{ft,rail} = \frac{\$Sand\_Blast}{1000\,ft,rail} x \frac{1}{1000} \tag{26}$$

$$\frac{\$Sand\_Blast}{1000\,ft,rail} = \frac{\$Labor,Sand}{1000\,ft} + \frac{\$Mat'l,Sand}{1000\,ft} + \frac{\$Misc,Sand}{1000\,ft} \tag{27}$$

$$\frac{ft,chips}{test} = \frac{ft,chipping,uncoated}{test} x(1-\%effectiveness) \tag{28}$$

The total cost information for each coating option is show in Table 15. According to ref [11], the remaining coating around a chipping area must also be removed before re-coating the damaged area by hand.

Table 15: Chipping Repair Cost of Sand and Water Blasting

Per Foot of Rail and Per Test

Chipping Repair / Maintenance	Uncoated	Iron Oxide	Epoxy	Units
Sand Blast	$0.00	$547.44	$551.88	per ft of rail
Water Blast	$0.00	$542.59	$544.11	per ft of rail
Sand Blast	$0.00	$36,883.80	$33,319.55	per test
Water Blast	$0.00	$36,556.77	$32,850.74	per test

The HHSTT uses two methods for removing material, sand and water blasting. In assessing total cost we will use the more expensive method, sand blasting. The cost difference per test is less than $500.00.

4.3.3 Failure

Failure is defined as catastrophic failure which requires rail and payload replacement. The payload's, or test set-up's, delivery is the purpose of the HHSTT. No assumption for payload replacement value was made and a range of values will be presented to show at what point it becomes cost effective to coat the rail and what distribution to use. Approximately two sections, or 78 feet, of rail are damaged beyond repair any time a failure occurs. The coating effectiveness factor is used here to reduce the frequency of failure. For instance, the baseline case fails every 12 tests. When using the epoxy it figures that the tests fail about every 17 tests. The replacement cost is then divided among those 17 tests. The rail replacement cost is also broken up among the 17

tests. The total cost each time a failure occurs is shown below and broken down to a cost

per failure and then to a cost per test dependant on what coating is used. below are

equations typical for both coatings.

$$\frac{\$Failure}{Test} = \frac{\$Mat'l\_replacement}{failure} x\frac{1\,failure}{\#tests} x\left(1-\%\,effectiveness\right) \tag{29}$$

$$\frac{\$Mat'l\_replacement}{failure} = \frac{\$Rail\_replacement}{failure} + \frac{\$Test\_set-up}{failure} \tag{30}$$

$$\frac{\$Rail\_replacement}{failure} = \frac{\$labor, rail}{failure} + \frac{\$mat'l, rail}{failure} \tag{31}$$

$$\frac{\$labor, rail}{failure} = \left(\#workers\right) x\frac{\$wage}{man \cdot hr} x\frac{\#days, install\,\&\,align}{failure} x\frac{8hr}{day} \tag{32}$$

$$\frac{\$mat'l, rail}{failure} = \frac{\$rail}{section} x\frac{\#section, replace}{failure} + \frac{\$coat, initial}{ft, rail} x\frac{\#section, replace}{failure} x\frac{39\,ft}{section} \tag{33}$$

The results of these equations for each coating are:

Table 16: Replacement Cost of Failure per Test for the Given Coating Conditions

Failure	Uncoated	Iron Oxide	Epoxy	Units
Cost of Failure	$0.00	$0.00	$58,659.12	per test

Where the replacement cost for oxide is zero because epoxy was used and it was assumed

that failure occurred in the epoxy coated area of the test track. These numbers will vary

depending on coating choice.

4.4 Cost per Test

The total cost per test to the DOD is the sum of the cost for a new coating plus chipping repair plus failure replacement cost per test.

$$\frac{\$Total}{test} = \frac{\$Failure}{test} + \frac{\$Chipping}{test} + \frac{\$New\_Coat}{test} \qquad (34)$$

The total cost summary shown in Table 17 breaks down the cost per test for various coatings.

Table 17: Total Cost to DOD Per Test for Given Coating

Covering the Entire Test Track

Total Cost per Test			
Test Set-up cost	All Uncoated	All Iron Oxide	All Epoxy
$500,000.00	$43,333.33	$95,379.23	$102,448.95
$1,000,000.00	$85,000.00	$127,462.57	$131,198.95
$2,000,000.00	$168,333.33	$191,629.23	$188,698.95
$3,000,000.00	$251,666.67	$255,795.90	$246,198.95
$4,000,000.00	$335,000.00	$319,962.57	$303,698.95
$5,000,000.00	$418,333.33	$384,129.23	$361,198.95
$6,000,000.00	$501,666.67	$448,295.90	$418,698.95

Figure 35 shows when it becomes economical to use a coating if you're coating the entire track.

Cost of Completely Coated Track per Test vs. Payload Value
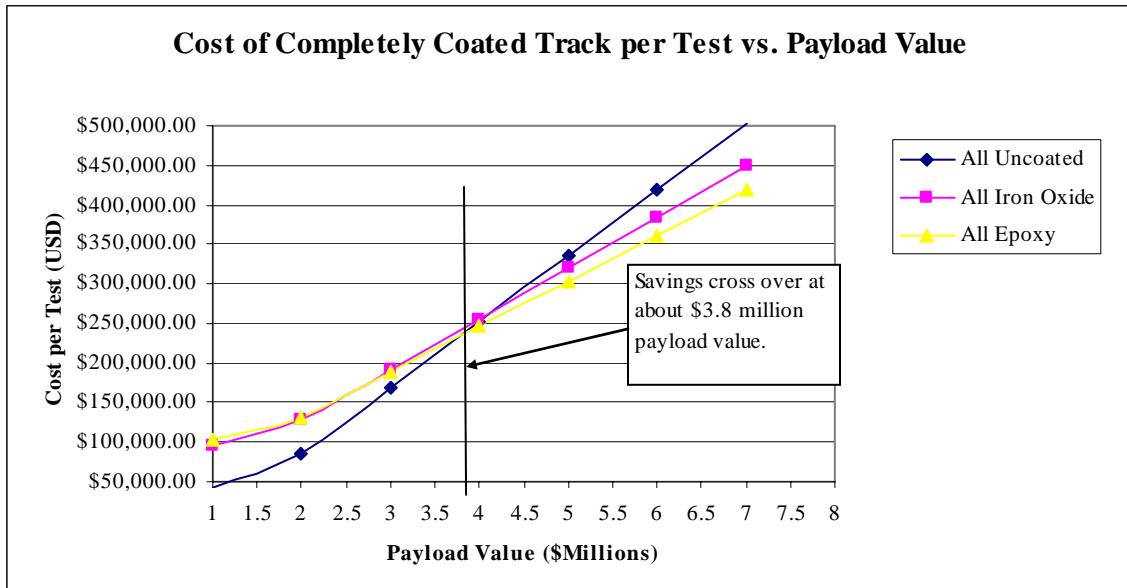
Figure 35: Cost per Test to the DOD for Single coating/uncoated on Entire Length of Test Track

If the entire rail is coated then it is reasonable to coat the rail when the payload replacement cost is above about $3.8 million.

What the HHSTT found, which seems to work best, is to break up the coating up into sections. The cost comparison supports that idea. The cost breakdown for some combinations of coatings thought to represent a spread of possibilities is shown in Table 1.

Again, it is assumed that the uncoated section, if present, is in the first portion of the track and that oxide coating precedes epoxy if both are present.

Table 18: Total Cost to the DOD per Test for Given Coating

Covering a State Section of the Test Track

Total Cost per Test			
Test Set-up cost	1/3 Each	2/3 Oxide	2/3 Epoxy
$500,000.00	$90,804.96	$91,570.99	$93,500.81
$1,000,000.00	$119,554.96	$123,654.32	$122,250.81
$2,000,000.00	$177,054.96	$187,820.99	$179,750.81
$3,000,000.00	$234,554.96	$251,987.66	$237,250.81
$4,000,000.00	$292,054.96	$316,154.32	$294,750.81
$5,000,000.00	$349,554.96	$380,320.99	$352,250.81
$6,000,000.00	$407,054.96	$444,487.66	$409,750.81

This is shown graphically here:
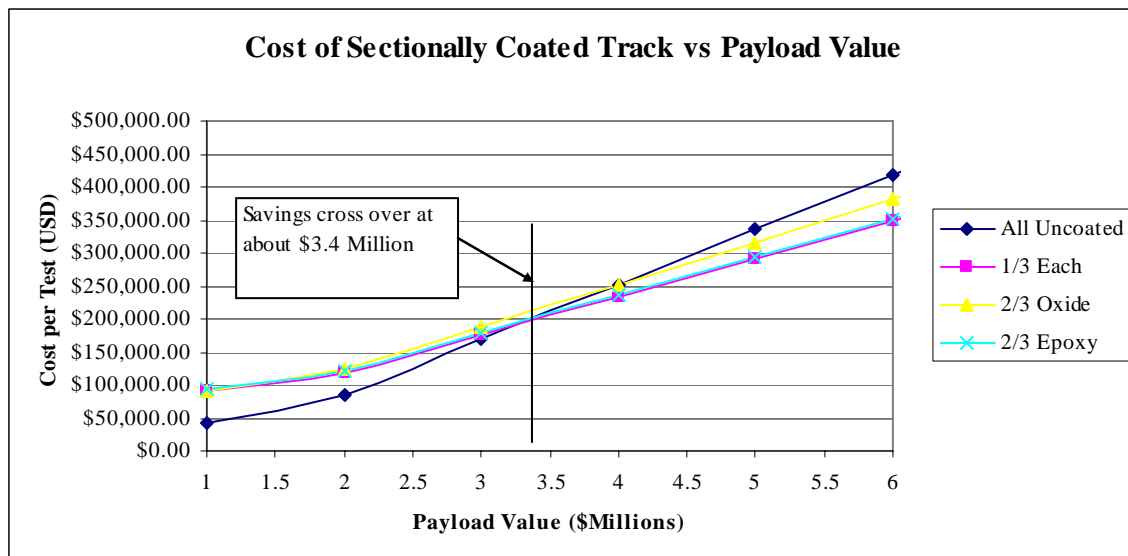
Figure 36: Cost per Test to the DOD, Sectionally Coated Track as Stated

For this test profile when the payload replacement cost is above about $3.3 to $3.4 million it is economical to use a coating. The most efficient of which is the 2/3 of epoxy coating. The advantage of this method, despite being slightly more expensive, is that only one coating is needed. It would save the preparation and clean-up time of coating with multiple types.

It must be remembered that this is for one test profile, speed and payload. If the velocity is increased then the sled failure rate will increase dramatically for an uncoated rail. This means that the coatings will have a more significant effect. The 31% effectiveness of epoxy will have a higher savings value over an uncoated or oxide coated rail.

Chapter 5 – Conclusions and Recommendations

5.1 Conclusions

At a 130 m/s impact velocity, CTH verified all experimental results within 14% for both coatings. At lower velocities the CTH Taylor Impact Test model holds. As velocity was increased, confidence in the results diminished because the 1080 projectile mixed in the cells with the coating and target material at the point of impact. CTH did still hold to the trend seen in experimental results. That trend was a greater radial deformation when using epoxy over oxide. Oxide had a greater radial deformation than an uncoated projectile. Based on these experimental results, verified by CTH at low velocities, the coating effectiveness factor, 31% for epoxy and 23% for oxide, was then used to find the most cost efficient coating.

From Figure 35 and Figure 36, we saw that epoxy is consistently the best choice for high value payloads. The cost of using only epoxy on the last portion of the rail may be the most efficient depending on the utility of coating the same amount of rail with all one coating versus breaking it up into two sections of different coatings. Using all epoxy would eliminate the necessity of using two different coatings. Also, using just one coating, it can be started wherever gouging is expected, generally where the sled velocity exceeds 1.5 km/second.

As the velocity of the HHSTT is pushed toward its goal of 10,000 ft/s, and beyond, the epoxy is clearly the optimum coating. Epoxy's advantage over oxide will have a more significant cost savings as test velocity, and also the amount of damage to an equivalent uncoated rail, increases.

5.2 Recommendations for Future Research

Further testing of material properties is needed to completely model the coatings to be used in CTH. Initial research was focused on finding stronger, harder materials to coat the rail and/or sled shoe. Results suggest that a softer, less brittle material is what is needed for a sacrificial rail coating to absorb the impact energy studied here. Material interfaces have proven to be an area of great concern when using an Eulerian Mesh based finite element code especially when the majority of the velocity is perpendicular to the boundary layer. For the Taylor Impact Test models, high velocity tests should be reconsidered so that they agree with experimental results.

The ideal coating is applied to shoe of the sled and not the rail. Difficulties arise in finding such a material that will not shear off when applied in sufficient thicknesses to protect the shoe from the temperatures and pressures seen at the HHSTT. Finding such a coating is the ultimate goal for the HHSTT. Currently, finding one that will work when coated to the rail will be sufficient to reach the goal of 10,000 ft/s.

Taylor Test Experimental Results

Uncoated 1080

	Test #	V_{impact} (m/s)	L_0 (mm)	L_1 (mm)	εL (%)	L_{UD} (mm)	L_{UD}/L_o
Uncoated 1080	S1	39	60.00	59.75	-0.42%	60	1.00
	S11	112	90.01	87.24	-3.08%	65.62	0.73
	S8	128	59.91	57.74	-3.62%	42.26	0.71
	S2	134	60.00	57.46	-4.23%	41.32	0.69
	S10	144	90.05	85.57	-4.98%	64.5	0.72
	S4	145	90.00	85.67	-4.81%	55.95	0.62
	S9	148	59.95	57.19	-4.60%	39.96	0.67
	S6	156	30.00	28.44	-5.20%	17.1	0.57
	S5	207	29.96	27.44	-8.41%	16.44	0.55
	S3	218	30.00	27.35	-8.83%	14.43	0.48
	S7	263	30.00	25.94	-13.53%	11.29	0.38

Uncoated 1080 (cont'd)

	Test #	V_{impact} (m/s)	D_0 (mm)	D_1 (mm)	ε D (%)	Deformation	Duration (μs)
Uncoated 1080	S1	39	6.00	6.00	0.00	none	42
	S11	112	5.95	6.40	0.08	Mushroom	84
	S8	128	6.00	6.52	0.09	Mushroom	63
	S2	134	6.00	6.60	0.10	Mushroom	63
	S10	144	5.92	6.82	0.15	Mushroom/buckle	105
	S4	145	5.90	6.60	0.12	Mushroom/buckle	84
	S9	148	5.89	6.60	0.12	Mushroom	63
	S6	156	6.00	6.97	0.16	Mushroom	42
	S5	207	6.00	7.90	0.32	Mushroom	42
	S3	218	6.00	8.10	0.35	Mushroom	63
	S7	263	6.01	9.59	0.60	Mushroom/fracture	63

Oxide Coated 1080

	Test #	V_{impact} (m/s)	L_0 (mm)	L_1 (mm)	εL (%)	L_{UD} (mm)	L_{UD} / L_o
Oxide 1080	I3	110	90.21	87.38	-0.03	54.40	0.60
	I2	130	60.19	57.90	-0.04	37.40	0.62
	I5	144	60.25	57.25	-0.05	32.25	0.54
	I1	161	30.32	28.61	-0.06	15.85	0.52
	I4	243	30.28	26.25	-0.13	10.70	0.35

Oxide Coated 1080 (cont'd)

	Test #	V_{impact} (m/s)	D_0 (mm)	D_1 (mm)	εD (%)	Deformation	Duration (μs)
Oxide 1080	I3	110	5.93	6.44	0.09	Mushroom	63
	I2	130	5.92	6.65	0.12	Mushroom	63
	I5	144	5.85	6.74	0.15	Mushroom	63
	I1	161	5.98	7.18	0.20	Mushroom	63
	I4	243	5.93	9.70	0.64	Mushroom/fracture	63

Epoxy Coated 1080

	Test #	V_{impact} (m/s)	L_0 (mm)	L_1 (mm)	εL (%)	L_{UD} (mm)	L_{UD} / L_o
Epoxy 1080	E3	108	90.55	87.68	-0.03	78.85	0.87
	E2	128	60.55	57.97	-0.04	47.00	0.78
	E5	144	60.48	57.37	-0.05	39.40	0.65
	E1	151	30.53	28.70	-0.06	20.80	0.68
	E4	243	30.51	26.31	-0.14	14.25	0.47

Epoxy Coated 1080 (cont'd)

	Test #	V_{impact} (m/s)	D_0 (mm)	D_1 (mm)	εD (%)	Deformation	Duration (µs)
Epoxy 1080	E3	108	5.96	6.41	0.08	Mushroom	84
	E2	128	5.96	6.65	0.12	Mushroom	63
	E5	144	5.97	6.90	0.16	Mushroom	63
	E1	151	6.04	7.13	0.18	Mushroom	42
	E4	243	5.97	10.20	0.71	Mushroom/fracture	63

CTH Input Deck – Taylor Impact Model, Epoxy Coated 1080 Steel

Note: Inputs shown in parentheses are values used for Oxide coated 1080.

```
*eor* genin

Taylor Test: Epoxy/1080 Steel Cylinder, Blint, V=130m/s

control
  mmp
  ep
  vpsave
endcontrol


*******************
*Mesh Generation
*******************
mesh
  block 1  geom=2dc    type=e   *  2dc is two dimensional cylindrical
                               *  e is for an Eulerian solution

    x0=0.0
      x1  n=225  w=0.45  dxf=0.002
      x2  n=20   w=0.15  dxf=0.0075
      x3  n=54   w=5.40  dxf=0.100
    endx
    y0=-6.0
      y1  n=59   w=5.90  dyf=0.100
      y2  n=795  w=1.59  dyf=0.002
      y3  n=50   w=5.00  dyf=0.100        *270296 cells
    endy
      xaction=0., 0.50            *Initial Calculation begins with
      yaction=-1., 6.020          *all cells within this range
  endb
endmesh
```

```
*****************************************
*Material Size, Location and Velocity
*****************************************
insertion of material

   block 1
     package cylinder
       material 1
       numsub 100
       yvel -130e2            *change only the first number, leave 'e2'
       insert box             *this converts m/s to cm/s
         p1 0.000 0.020
         p2 0.300 6.020
       endinsert
     endpackage

     package coating_disc    *Coating around projectile
                             *of 0.02cm thick.
       material 2
       numsub 100
       yvel -130e2
       insert box
       p1 0.000 0.000
       p2 0.300 0.020
       endinsert
     endpackage

     Package coating_cyl
       material 2
       numsub 100
       yvel -130e2
       insert box
       p1 0.300 0.000
       p2 0.320 6.020
       endinsert
     endpackage

     Package Target
      material 3
      numsub 100
      insert box
      p1 0.000 0.000
      p2 6.000 -6.00
      endinsert
     endpackage
   endblock
endinsertion
```

```
*************************
*Tracer Point Insertions
*************************
tracer

*Final Length and Diameter
****************************************
*1 Cylinder Top Center (Deformed Length)
     add 0.00 6.020
*2 Cylinder Bottom Center
     add 0.00 0.021
*3 Cylinder Bottom Edge
     add 0.299 0.021
*4 Cylinder 0.25cm up from base
     add 0.299 0.27

*Profile Approximators, Undeformed Length
******************************************
*5 Cylinder Edge 0.50cm
     add 0.299 0.52
*6 Cylinder Edge 0.75cm
     add 0.299 0.77
*7 Cylinder Edge 1.00cm
     add 0.299 1.02
*8 Cylinder Edge 1.50cm
     add 0.299 1.52
*9 Cylinder Edge 2.00cm
     add 0.299 2.02
*10 Cylinder Edge 2.50cm
     add 0.299 2.52
*11 Cylinder Edge 3.00cm
     add 0.299 3.02
*12 Cylinder Edge 4.00cm
     add 0.299 4.02
*13 Cylinder Edge 5.00cm
     add 0.299 5.02
*14 Cylinder Edge 6.00cm
     add 0.299 6.02

*Center Line Properties   (also includes tracer points 1 and 2)
*************************
*15 Cylinder Center
     add 0.00 1.02
*16 Cylinder Center
     add 0.00 2.02
*17 Cylinder Center
     add 0.00 3.02
*18 Cylinder Center
     add 0.00 4.02
*19 Cylinder Center
     add 0.00 5.02
```

```
*Coating Properties at Cylinder Face
************************************
*20 Coating Mid-Point
      add 0.00 0.01
*21 Coating Mid-Point
      add 0.15 0.01
*22 Coating Mid-Point
      add 0.30 0.01
endt




**********************
*Equations of State
**********************
eos
   MAT1 SES IRON                      *Iron approximation for 1080 Steel
   MAT2 MGR EPOXY_RESIN1              *(MAT2 SES IRON)
   MAT3 SES STEEL_V300
endeos




*********************
*Material Properties
*********************
epdata
   mix = 3

   matep 1 JO USER           *Kennan coefficients for 1080 steel.
      ajo= 5.25e9 *Dynes/cc
      bjo= 35.9e9 *Dynes/cc
      cjo= 2.9e-2
      mjo= 6.74e-1
      njo= 0.6677
      tjo= .1591885e-1
      poisson= 0.283

   matep 2 *EPOXY COATING (HEMATITE)
      Yield=0.1e8  *           (0.5e7)
      Poisson=0.46 *           (0.26)

   matep 3 ST V-250_STEEL
```

68

```
      *******************************
      *Material Interface Conditions
      *******************************
      Blint 1                        *Creates a frictional boundary layer
         hard 3                      *between the coating and VascoMax
         soft 2

          *Friction Coefficient
          *********************
          fric 0.3 *[Tech Report #TR97-3]  (0.6)

endep

*Boundary condition preceded by "*" input indicated a "No Slip"
*condition




****************************************************
*eor* cthin

Taylor Test: Epoxy/1080 Steel Cylinder, Blint, V=130m/s


*********************
*Simulation Run Time
*********************
control
  tstop = 85.0e-6                *Maximum time of contact with target.
endc                             *observed in lab.

restart
   nu=1
endr

Convct
 convection=1
 interface=high_resolution
endc


***********************
*Fracture Press Inputs
***********************
fracts

 pfrac1 -10.6e9   *$\sigma_U$ for material 1
 pfrac2 -0.1e8    *Must be at least equal to yield (0.5e7)
 pfmix  -12.0e9
 pfvoid -12.0e9
endf
```

69

```
************************************
*Time Cycle for Finite Differencing
************************************
edit
  shortt
    time = 0.0,   dt = 0.5e-6        *Take all data points every 0.5 μs
  ends
  longt
    time = 0.0,   dt = 1.0
  endl

  histt
    time = 0.0,   dt = 0.5e-6
    htracer all
  endh

  plott
    time = 0.0,   dt = 0.5e-6
  endp
ende


*********************
*Mesh Boundary Conditions
*********************
boundary
   bhydro  * rigid boundaries all around
     bl 1
       bxb = 0 , bxt = 0
       byb = 0 , byt = 0      *byb=1 was found to cause a breakdown
     endb                     *of the projectile into a liquid upon
                              *impact.
   endh
endb

cellthermo
 mmp
 tbad = 5000000         *Number of allowable thermodynamic errors
endc
```

Appendix 3

CTH Tracer Point Results

Epoxy, No Slip, V = 130 m/s, Fracture Pressure = 1.5e8 Dyne / cc

Coating Pressure, Tracer = 21

Taylor Test: Epoxy/1080 Steel Cylinder, No Slip, V=130m/s
EPOANZ   5/16/05   14:39:18   CTH
L POINT 21

Coating Pressure, Tracer = 22

Taylor Test: Epoxy/1080 Steel Cylinder, No Slip, V=130m/s
EPOANZ   5/16/05   14:39:18   CTH
L POINT 22

Epoxy, Boundary Layer, V = 130 m/s, Fracture Pressure = 1.5e8 Dyne / cc

75

Coating Temperature, Tracer = 21

Taylor Test: Epoxy/1080 Steel Cylinder, Blint, V=130m/s
EQQCCC   5/17/05   22:22:16   CTH
L POINT 21

Coating Temperature, Tracer = 22

Taylor Test: Epoxy/1080 Steel Cylinder, Blint, V=130m/s
EQQCCC   5/17/05   22:22:16   CTH
L POINT 22

1080 Pressure, Center, Tracer = 2

Taylor Test: Epoxy/1080 Steel Cylinder, Blint, V=130m/s
EQQCCC   5/17/05   22:22:16   CTH
L POINT 2

1080 Pressure, Center, Tracer = 15

Taylor Test: Epoxy/1080 Steel Cylinder, Blint, V=130m/s
EQQCCC   5/17/05   22:22:16   CTH
L POINT 15

1080 Pressure, Edge, Tracer = 3

Taylor Test: Epoxy/1080 Steel Cylinder, Blint, V=130m/s
EQQCCC   5/17/05   22:22:16   CTH
L POINT 3

1080 Pressure, Edge, Tracer = 7

Taylor Test: Epoxy/1080 Steel Cylinder, Blint, V=130m/s
EQQCCC   5/17/05   22:22:16   CTH
L POINT 7

77

Coating Pressure, Tracer = 20

Taylor Test: Epoxy/1080 Steel Cylinder, Blint, V=130m/s
EQQCCC   5/17/05   22:22:16   CTH
L POINT 20

Coating Pressure, Tracer = 21

Taylor Test: Epoxy/1080 Steel Cylinder, Blint, V=130m/s
EQQCCC   5/17/05   22:22:16   CTH
L POINT 21

Coating Pressure, Tracer = 22

Taylor Test: Epoxy/1080 Steel Cylinder, Blint, V=130m/s
EQQCCC   5/17/05   22:22:16   CTH
L POINT 22

78

Epoxy, No Slip, V = 130 m/s, Fracture Pressure = 1.0e7 Dyne / cc

Taylor Test: Epoxy/1080 Steel Cylinder, No Slip, V=130m/s, PFRAC=0.1e8
EWUEZN   5/24/05   02:37:39   CTH
L POINT 2

Taylor Test: Epoxy/1080 Steel Cylinder, No Slip, V=130m/s, PFRAC=0.1e8
EWUEZN   5/24/05   02:37:39   CTH
L POINT 3

Taylor Test: Epoxy/1080 Steel Cylinder, No Slip, V=130m/s, PFRAC=0.1e8
EWUEZN   5/24/05   02:37:39   CTH
L POINT 20

Taylor Test: Epoxy/1080 Steel Cylinder, No Slip, V=130m/s, PFRAC=0.1e8
EWUEZN   5/24/05   02:37:39   CTH
L POINT 21

Taylor Test: Epoxy/1080 Steel Cylinder, No Slip, V=130m/s, PFRAC=0.1e8
EWUEZN   5/24/05   02:37:39   CTH
L POINT 22

Epoxy, No Slip, V = 243 m/s, Fracture Pressure = 1.5e8 Dyne / cc

Edge Profile, Tracer = 12

Taylor Test: Epoxy/1080 Steel Cylinder, No Slip, V=243m/s
EQIEUD   5/17/05   09:27:18   CTH
L POINT 12

Edge Profile, Tracer = 13

Taylor Test: Epoxy/1080 Steel Cylinder, No Slip, V=243m/s
EQIEUD   5/17/05   09:27:18   CTH
L POINT 13

1080 Temperature, Center, Tracer = 2

Taylor Test: Epoxy/1080 Steel Cylinder, No Slip, V=243m/s
EQIEUD   5/17/05   09:27:18   CTH
L POINT 2

1080 Temperature, Edge, Tracer = 3

Taylor Test: Epoxy/1080 Steel Cylinder, No Slip, V=243m/s
EQIEUD   5/17/05   09:27:18   CTH
L POINT 3

1080 Pressure, Center, Tracer = 2

Taylor Test: Epoxy/1080 Steel Cylinder, No Slip, V=243m/s
EQIEUD   5/17/05   09:27:18   CTH
L POINT 2

1080 Pressure, Edge, Tracer = 3

Taylor Test: Epoxy/1080 Steel Cylinder, No Slip, V=243m/s
EQIEUD   5/17/05   09:27:18   CTH
L POINT 3

83

Taylor Test: Epoxy/1080 Steel Cylinder, No Slip, V=243m/s
EQIEUD   5/17/05   09:27:18   CTH
L POINT 20

Taylor Test: Epoxy/1080 Steel Cylinder, No Slip, V=243m/s
EQIEUD   5/17/05   09:27:18   CTH
L POINT 21

Taylor Test: Epoxy/1080 Steel Cylinder, No Slip, V=243m/s
EQIEUD   5/17/05   09:27:18   CTH
L POINT 22

Taylor Test: Epoxy/1080 Steel Cylinder, No Slip, V=243m/s
EQIEUD   5/17/05   09:27:18   CTH
L POINT 20

Taylor Test: Epoxy/1080 Steel Cylinder, No Slip, V=243m/s
EQIEUD   5/17/05   09:27:18   CTH
L POINT 21

Taylor Test: Epoxy/1080 Steel Cylinder, No Slip, V=243m/s
EQIEUD   5/17/05   09:27:18   CTH
L POINT 22

84

Epoxy, Boundary Layer, V = 243 m/s, Fracture Pressure = 1.5e8 Dyne / cc

Edge Profile, Tracer = 12
Taylor Test: Epoxy/1080 Steel Cylinder, Blint, V=243m/s
EQKFGS   5/17/05   11:33:58   CTH
L POINT 12

Edge Profile, Tracer = 13
Taylor Test: Epoxy/1080 Steel Cylinder, Blint, V=243m/s
EQKFGS   5/17/05   11:33:58   CTH
L POINT 13

1080 Temperature, Center, Tracer = 2
Taylor Test: Epoxy/1080 Steel Cylinder, Blint, V=243m/s
EQKFGS   5/17/05   11:33:58   CTH
L POINT 2

1080 Temperature, Edge, Tracer = 3
Taylor Test: Epoxy/1080 Steel Cylinder, Blint, V=243m/s
EQKFGS   5/17/05   11:33:58   CTH
L POINT 3

1080 Temperature, Edge, Tracer = 7
Taylor Test: Epoxy/1080 Steel Cylinder, Blint, V=243m/s
EQKFGS   5/17/05   11:33:58   CTH
L POINT 7

Coating Temperature, Tracer = 20
Taylor Test: Epoxy/1080 Steel Cylinder, Blint, V=243m/s
EQKFGS   5/17/05   11:33:58   CTH
L POINT 20

Coating Pressure, Tracer = 20

Taylor Test: Epoxy/1080 Steel Cylinder, Blint, V=243m/s
EQKFGS   5/17/05   11:33:58   CTH
L POINT 20

Coating Pressure, Tracer = 21

Taylor Test: Epoxy/1080 Steel Cylinder, Blint, V=243m/s
EQKFGS   5/17/05   11:33:58   CTH
L POINT 21

Coating Pressure, Tracer = 22

Taylor Test: Epoxy/1080 Steel Cylinder, Blint, V=243m/s
EQKFGS   5/17/05   11:33:58   CTH
L POINT 22

Oxide, No Slip, V = 130 m/s, Fracture Pressure = 1.5e8 Dyne / cc

89

Edge Profile, Tracer = 10

Taylor Test: Oxide/1080 Steel Cylinder, No Slip, V=130m/s
EPVAAN   5/16/05   21:35:01   CTH
L POINT 10

Edge Profile, Tracer = 11

Taylor Test: Oxide/1080 Steel Cylinder, No Slip, V=130m/s
EPVAAN   5/16/05   21:35:01   CTH
L POINT 11

1080 Temperature, Center, Tracer = 2

Taylor Test: Oxide/1080 Steel Cylinder, No Slip, V=130m/s
EPVAAN   5/16/05   21:35:01   CTH
L POINT 2

1080 Temperature, Edge, Tracer = 3

Taylor Test: Oxide/1080 Steel Cylinder, No Slip, V=130m/s
EPVAAN   5/16/05   21:35:01   CTH
L POINT 3

1080 Pressure, Center, Tracer = 2

Taylor Test: Oxide/1080 Steel Cylinder, No Slip, V=130m/s
EPVAAN   5/16/05   21:35:01   CTH
L POINT 2

1080 Pressure, Edge, Tracer = 3

Taylor Test: Oxide/1080 Steel Cylinder, No Slip, V=130m/s
EPVAAN   5/16/05   21:35:01   CTH
L POINT 3

Coating Temperature, Tracer = 20

Taylor Test: Oxide/1080 Steel Cylinder, No Slip, V=130m/s
EPVAAN   5/16/05   21:35:01   CTH
L POINT 20

Coating Temperature, Tracer = 21

Taylor Test: Oxide/1080 Steel Cylinder, No Slip, V=130m/s
EPVAAN   5/16/05   21:35:01   CTH
L POINT 21

Coating Temperature, Tracer = 22

Taylor Test: Oxide/1080 Steel Cylinder, No Slip, V=130m/s
EPVAAN   5/16/05   21:35:01   CTH
L POINT 22

Coating Pressure, Tracer = 20

Taylor Test: Oxide/1080 Steel Cylinder, No Slip, V=130m/s
EPVAAN   5/16/05   21:35:01   CTH
L POINT 20

Coating Pressure, Tracer = 21

Taylor Test: Oxide/1080 Steel Cylinder, No Slip, V=130m/s
EPVAAN   5/16/05   21:35:01   CTH
L POINT 21

Coating Pressure, Tracer = 22

Taylor Test: Oxide/1080 Steel Cylinder, No Slip, V=130m/s
EPVAAN   5/16/05   21:35:01   CTH
L POINT 22

Oxide, Boundary Layer, V = 130 m/s, Fracture Pressure = 1.5e8 Dyne / cc

92

Edge Profile, Tracer = 10

Taylor Test: Oxide/1080 Steel Cylinder, Blint, V=130m/s
EPOBKV   5/16/05   14:52:00   CTH
L POINT 10

Edge Profile, Tracer = 11

Taylor Test: Oxide/1080 Steel Cylinder, Blint, V=130m/s
EPOBKV   5/16/05   14:52:00   CTH
L POINT 11

1080 Temperature, Center, Tracer = 2

Taylor Test: Oxide/1080 Steel Cylinder, Blint, V=130m/s
EPOBKV   5/16/05   14:52:00   CTH
L POINT 2

1080 Temperature, Edge, Tracer = 3

Taylor Test: Oxide/1080 Steel Cylinder, Blint, V=130m/s
EPOBKV   5/16/05   14:52:00   CTH
L POINT 3

1080 Pressure, Center, Tracer = 2

Taylor Test: Oxide/1080 Steel Cylinder, Blint, V=130m/s
EPOBKV   5/16/05   14:52:00   CTH
L POINT 2

1080 Pressure, Edge, Tracer = 3

Taylor Test: Oxide/1080 Steel Cylinder, Blint, V=130m/s
EPOBKV   5/16/05   14:52:00   CTH
L POINT 3

Appendix 4

CTH Graphical Results

Epoxy, No Slip, V = 130 m/s, Fracture Pressure = 1.5e8 Dyne / cc

Taylor Test: Epoxy/1080 Steel Cylinder, No Slip, V=130m/s

EPOANZ   5/16/05 14:39:18 CTH   15721   Time=8.50051x10^{-5}

96
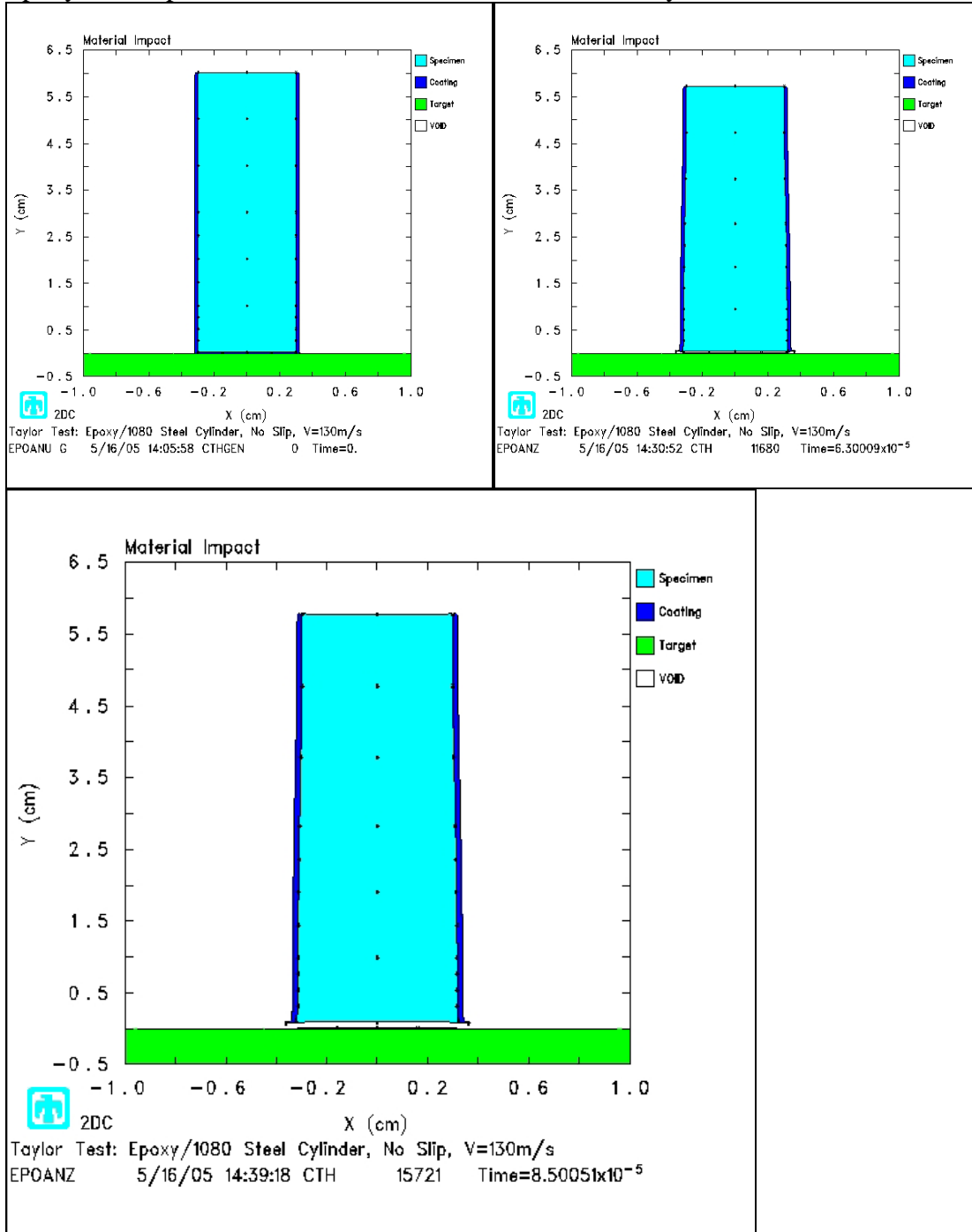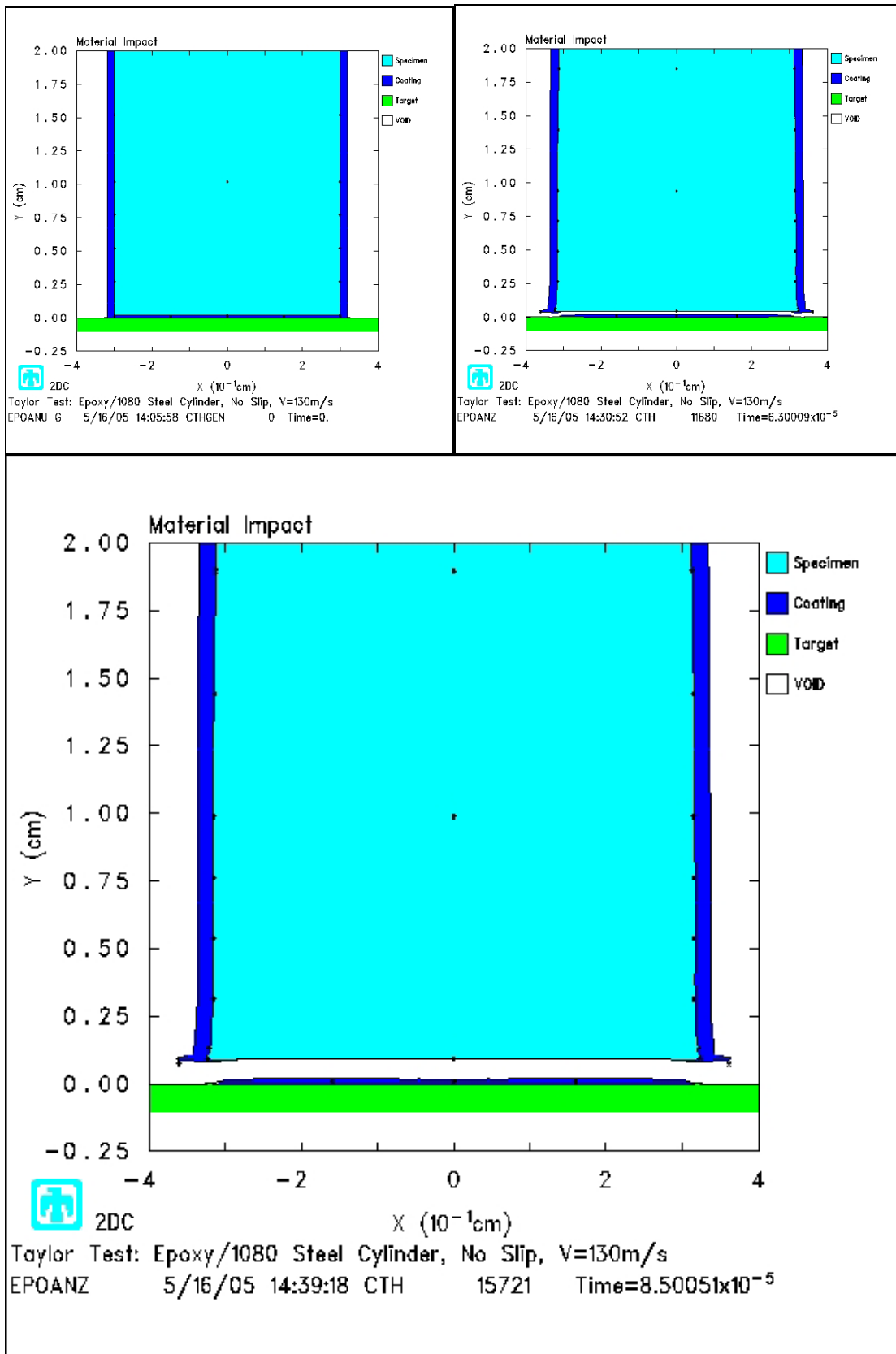
Epoxy, Boundary Layer, V = 130 m/s, Fracture Pressure = 1.5e8 Dyne / cc
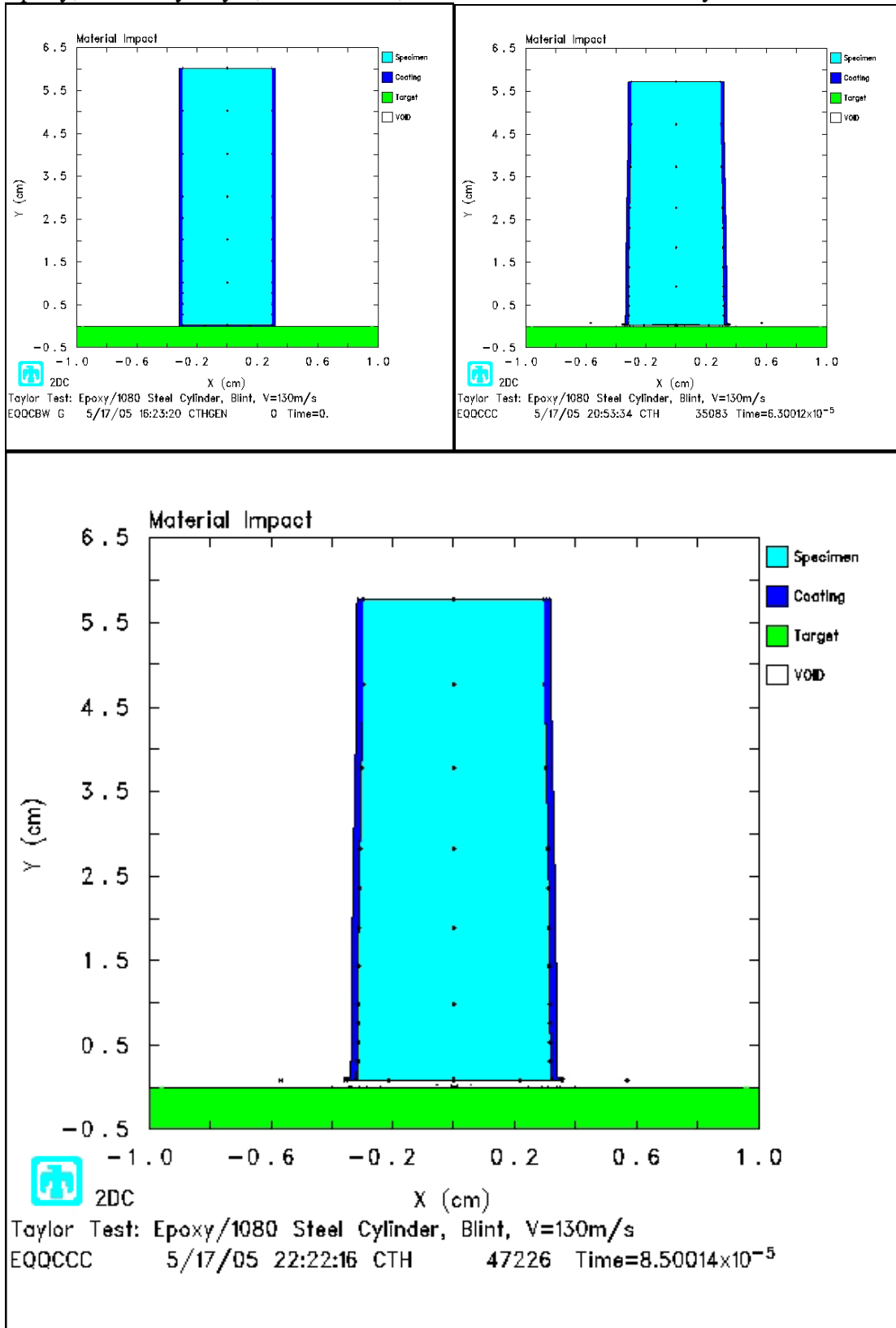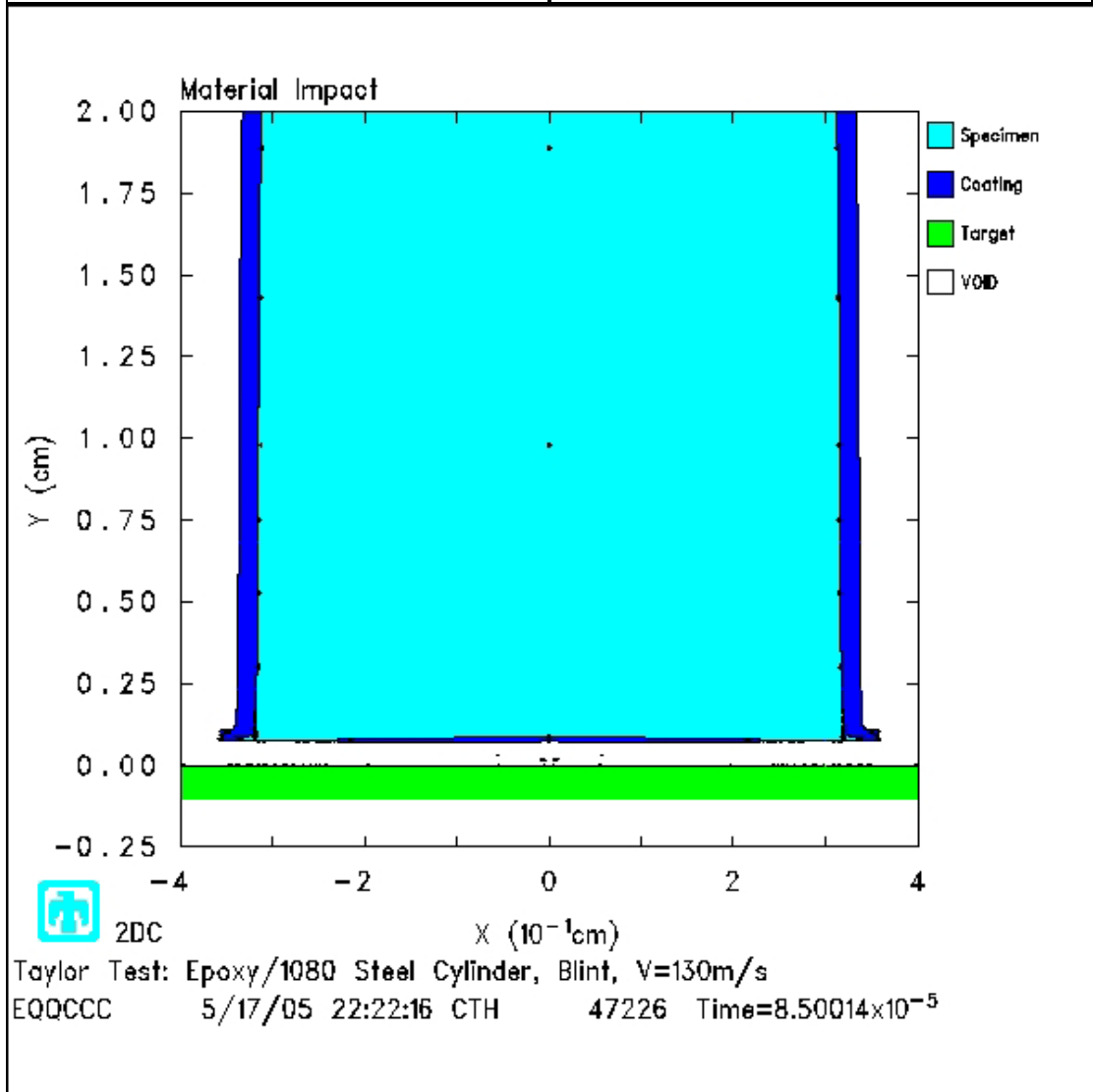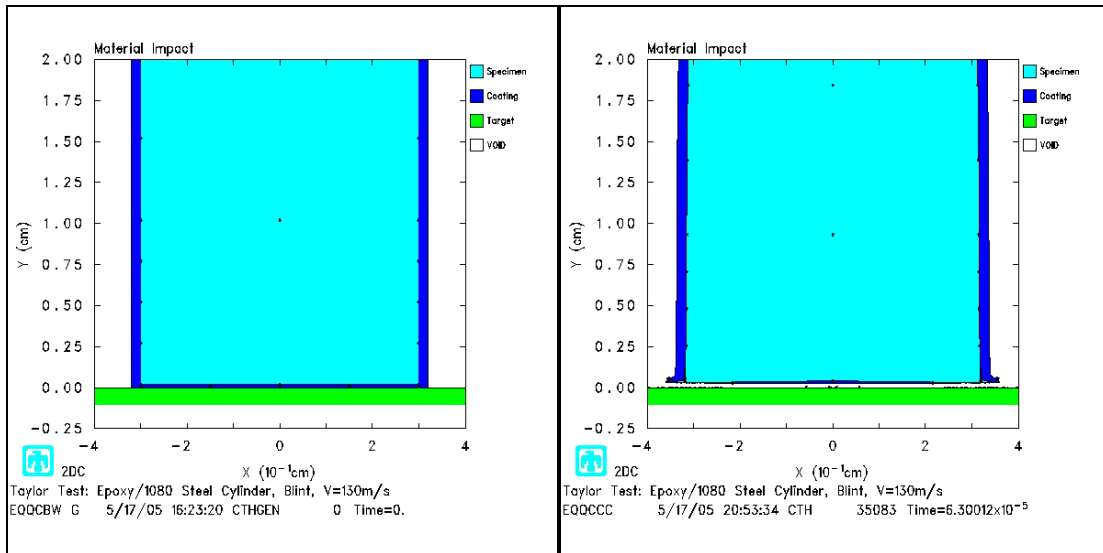
Epoxy, No Slip, V = 130 m/s, Fracture Pressure = 1.0e7 Dyne / cc
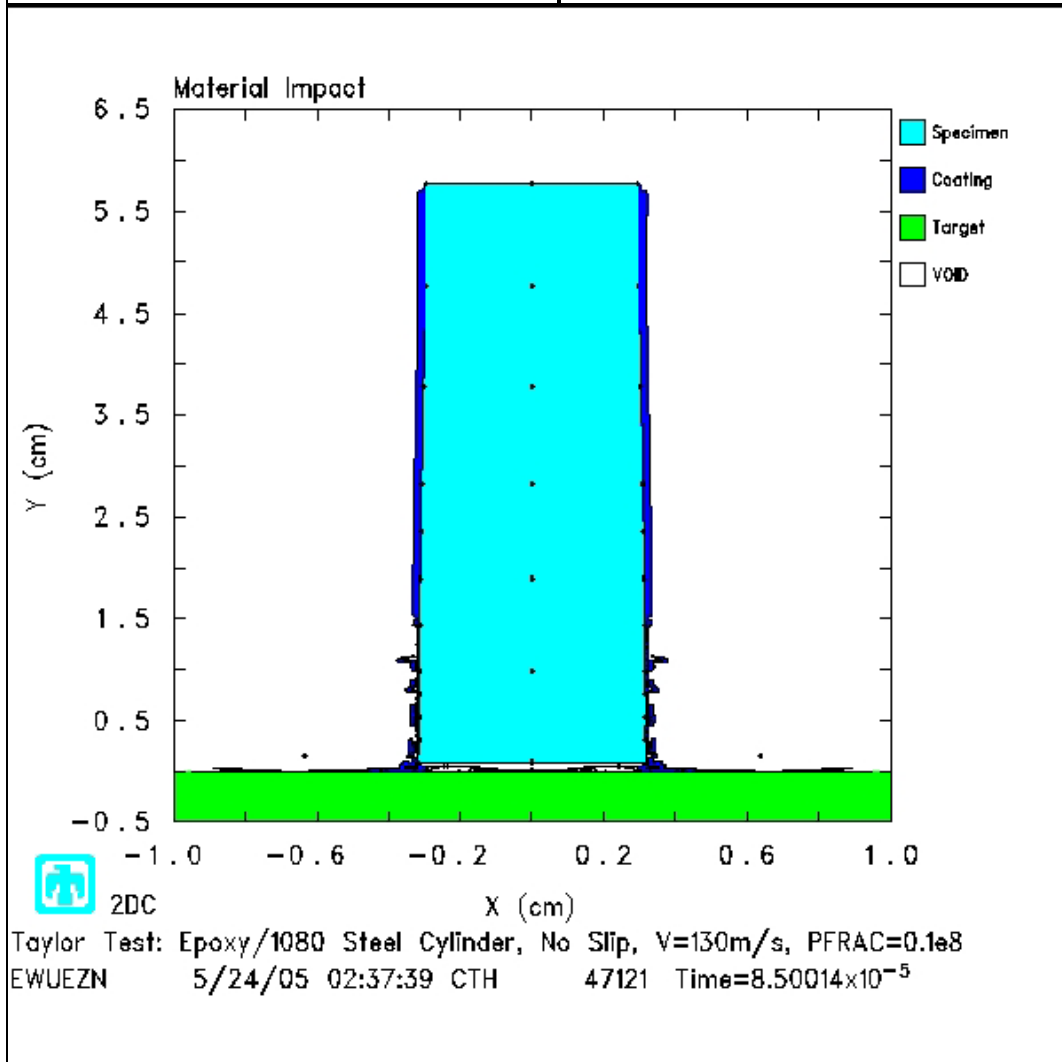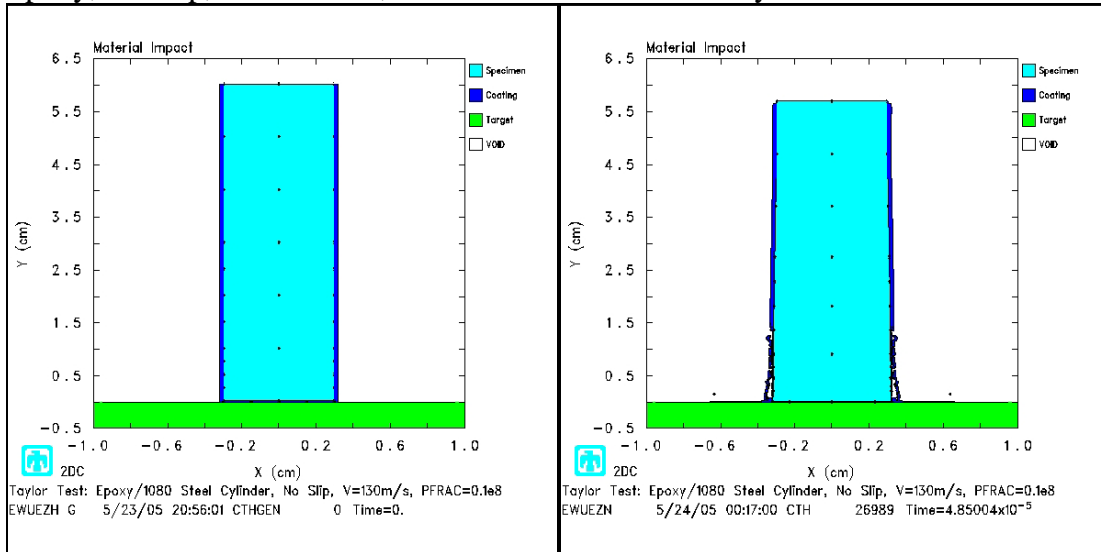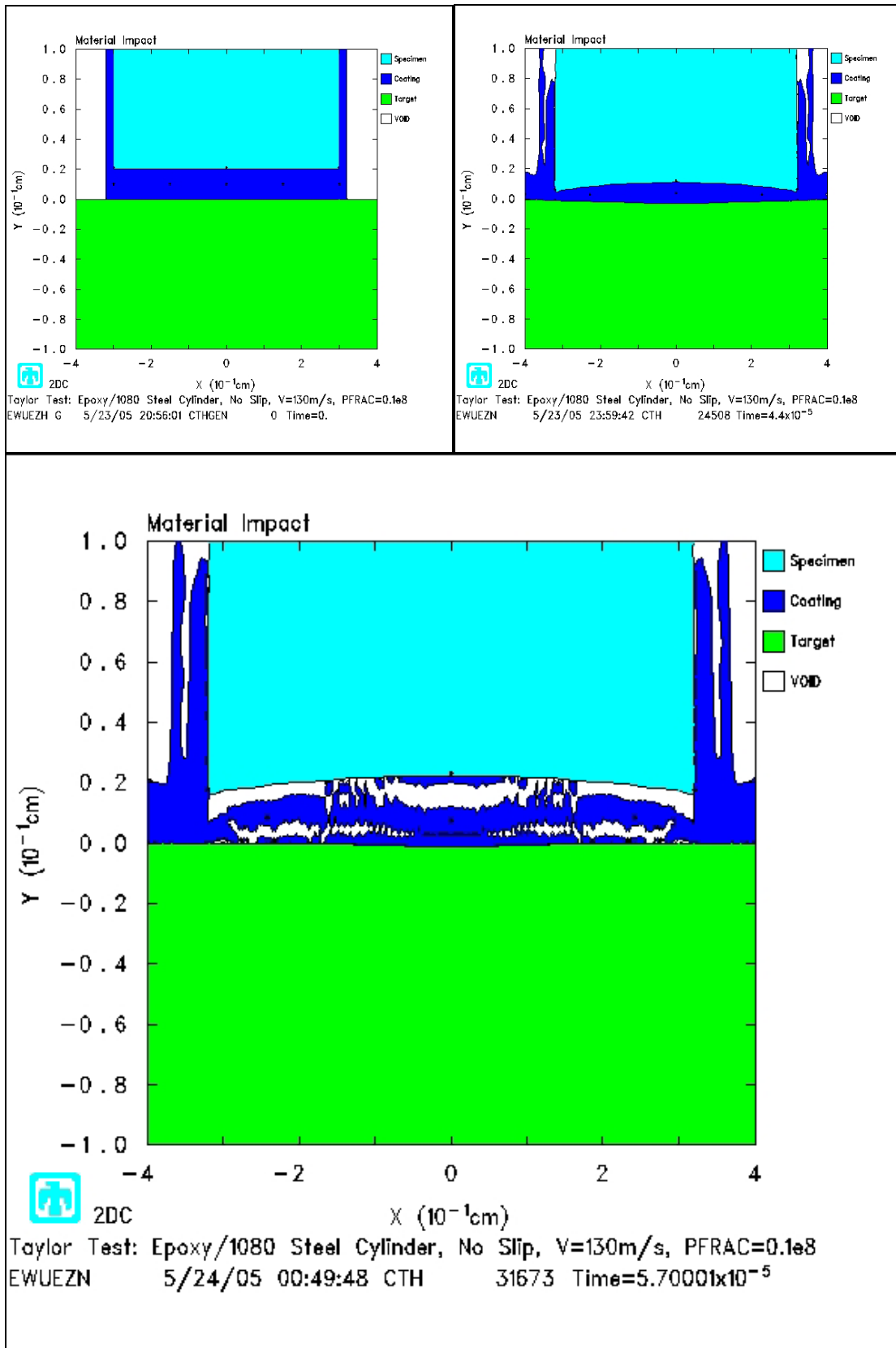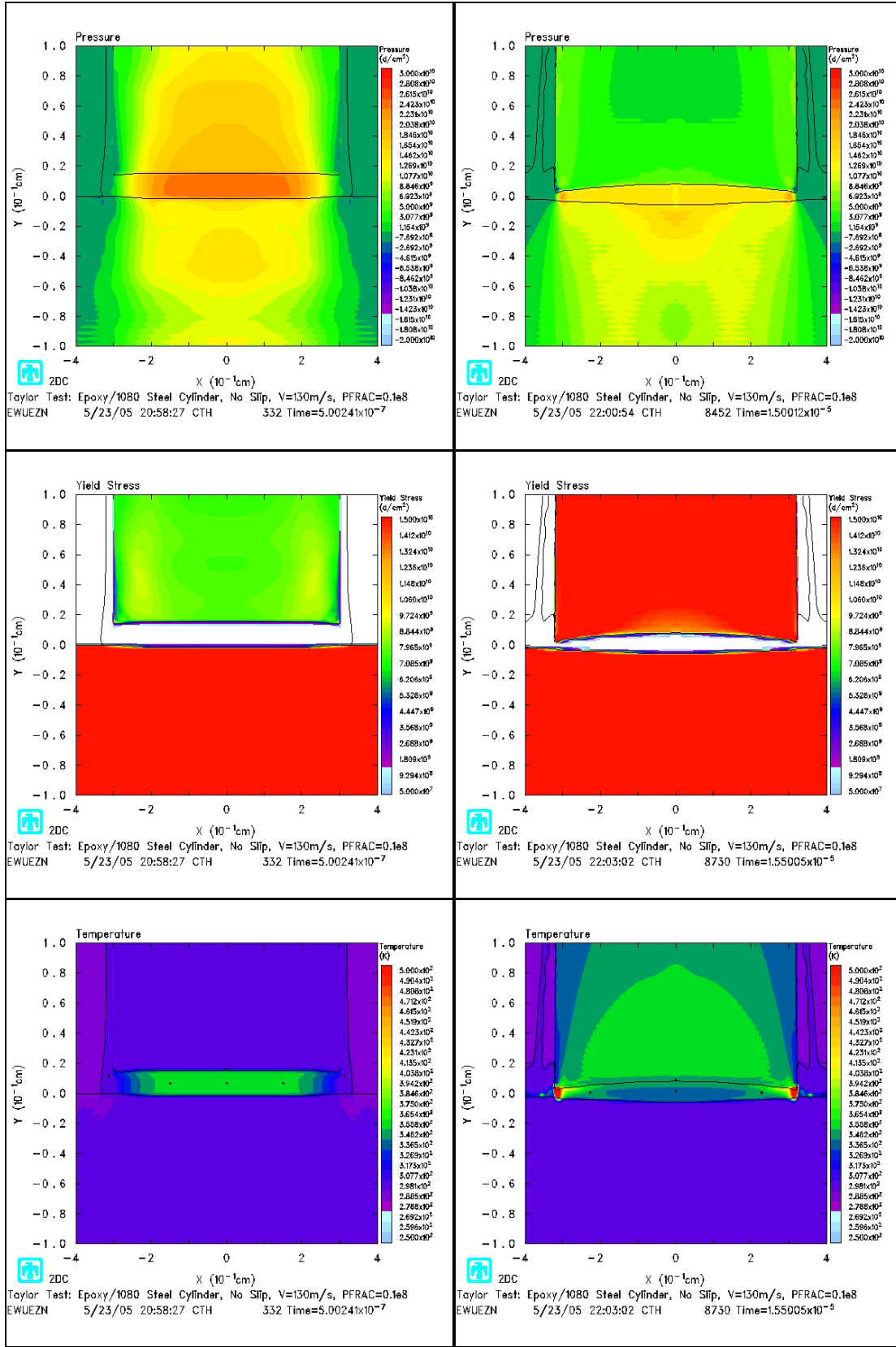
Epoxy, Boundary Layer, V = 130 m/s, Fracture Pressure = 1.0e7 Dyne / cc

103
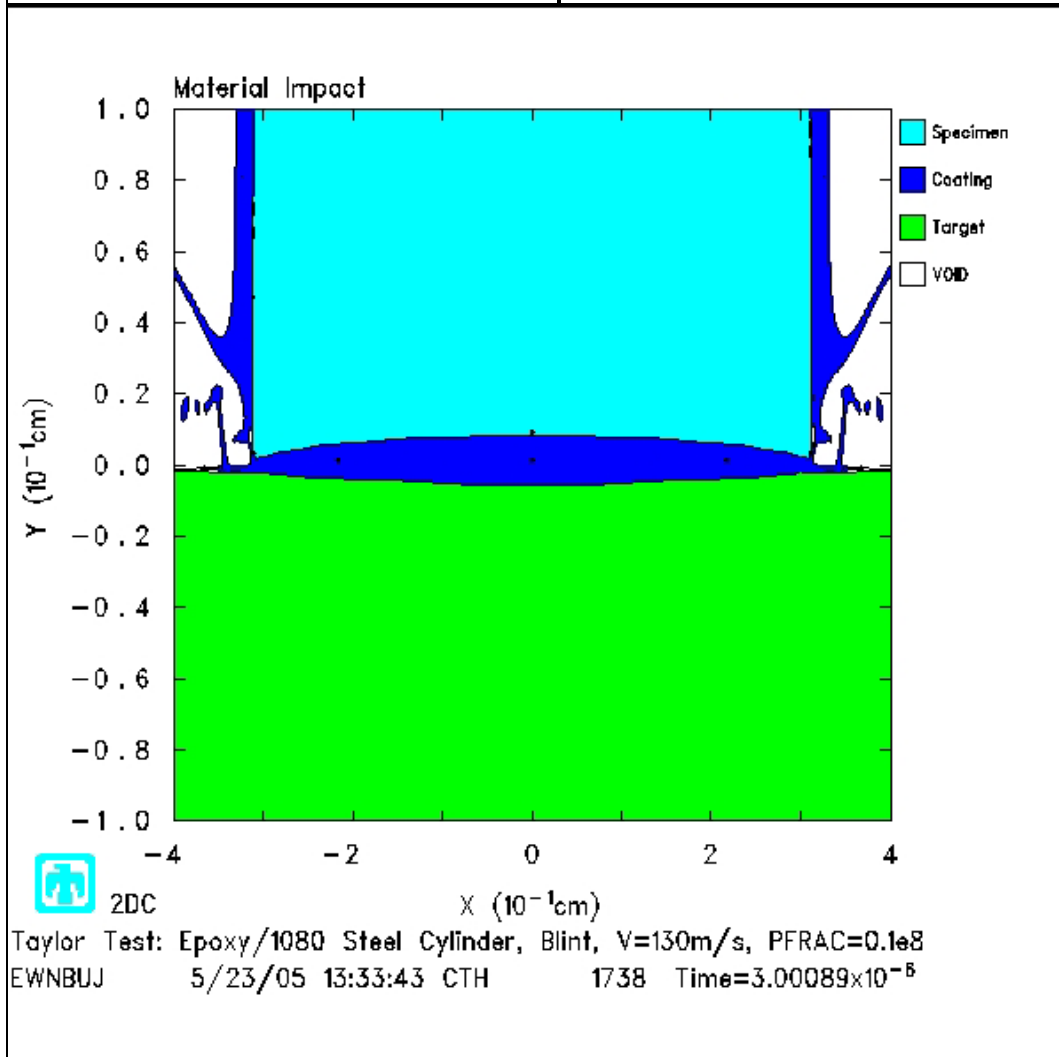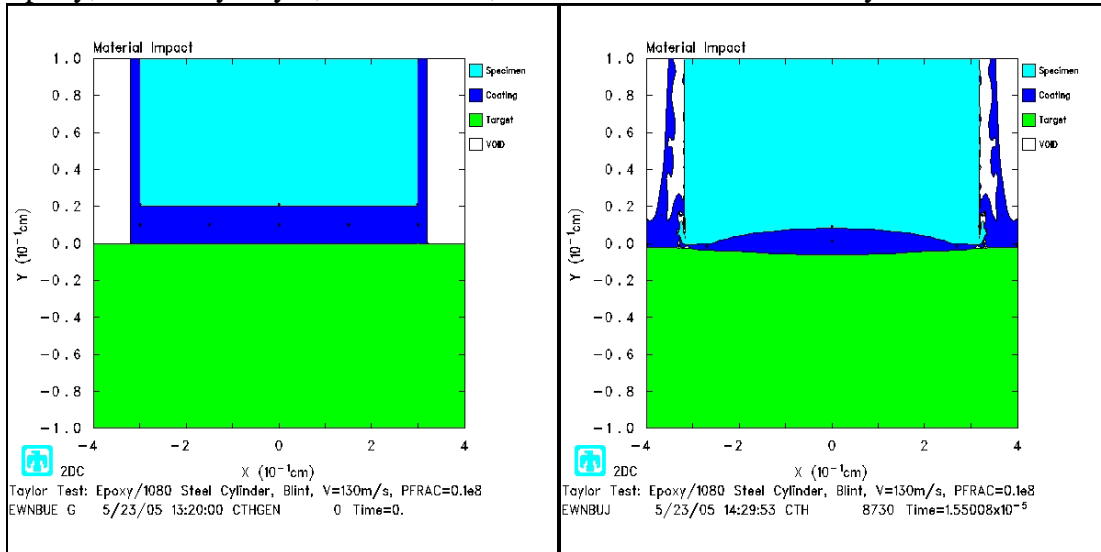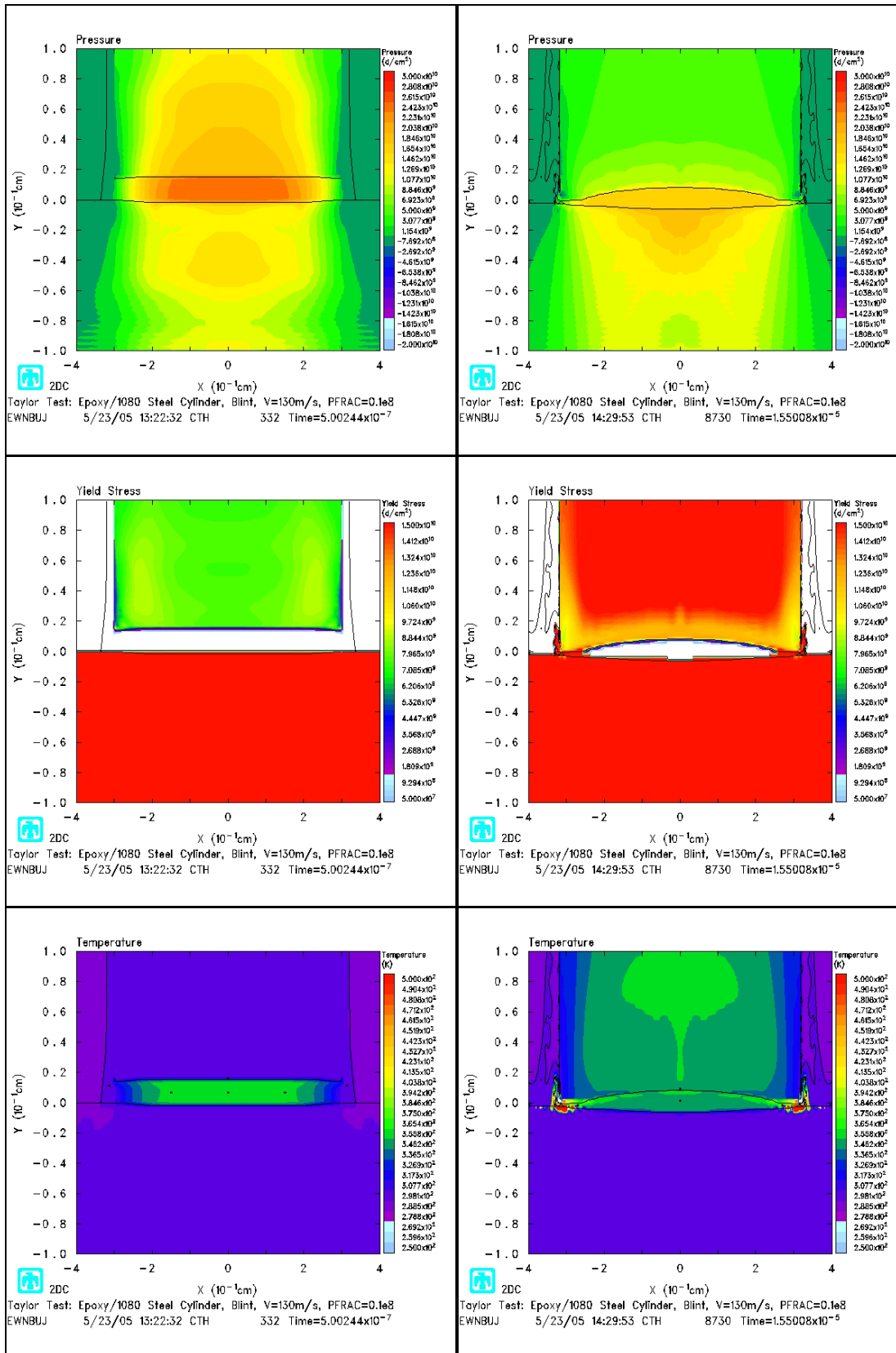
Epoxy, No Slip, V = 243 m/s, Fracture Pressure = 1.5e8 Dyne / cc
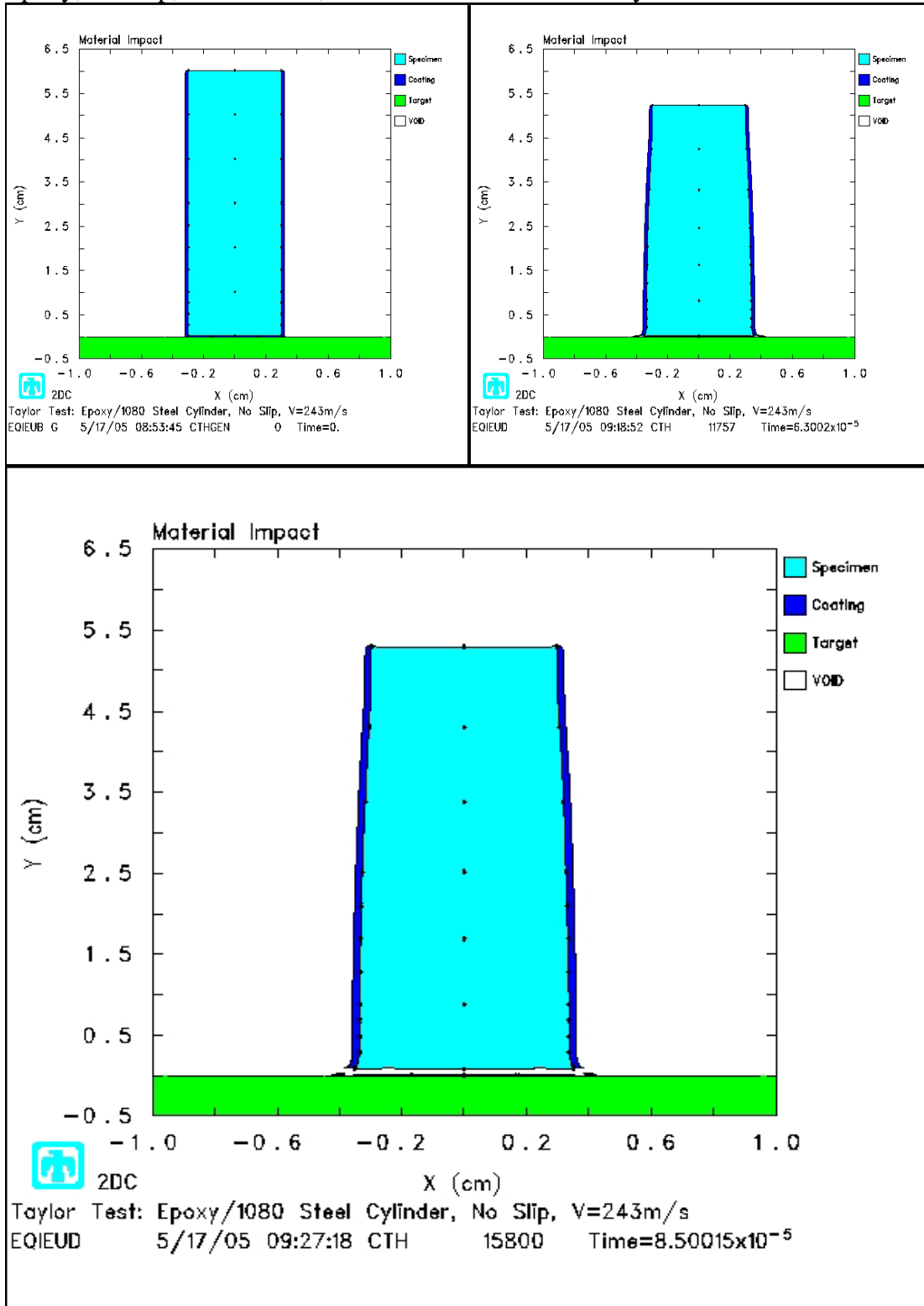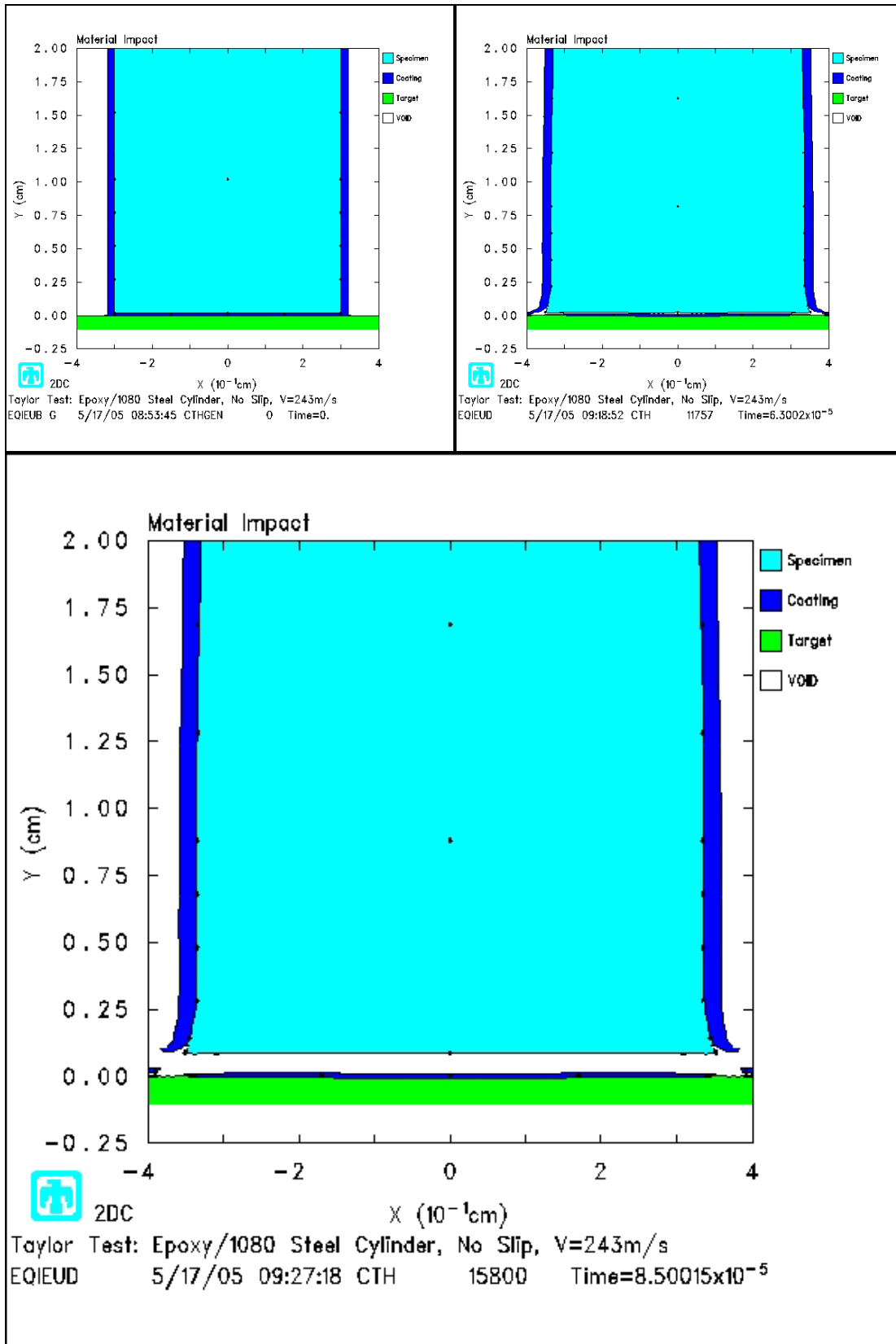
Epoxy, Boundary Layer, V = 243 m/s, Fracture Pressure = 1.5e8 Dyne / cc

Oxide, No Slip, V = 130 m/s, Fracture Pressure = 1.5e8 Dyne / cc
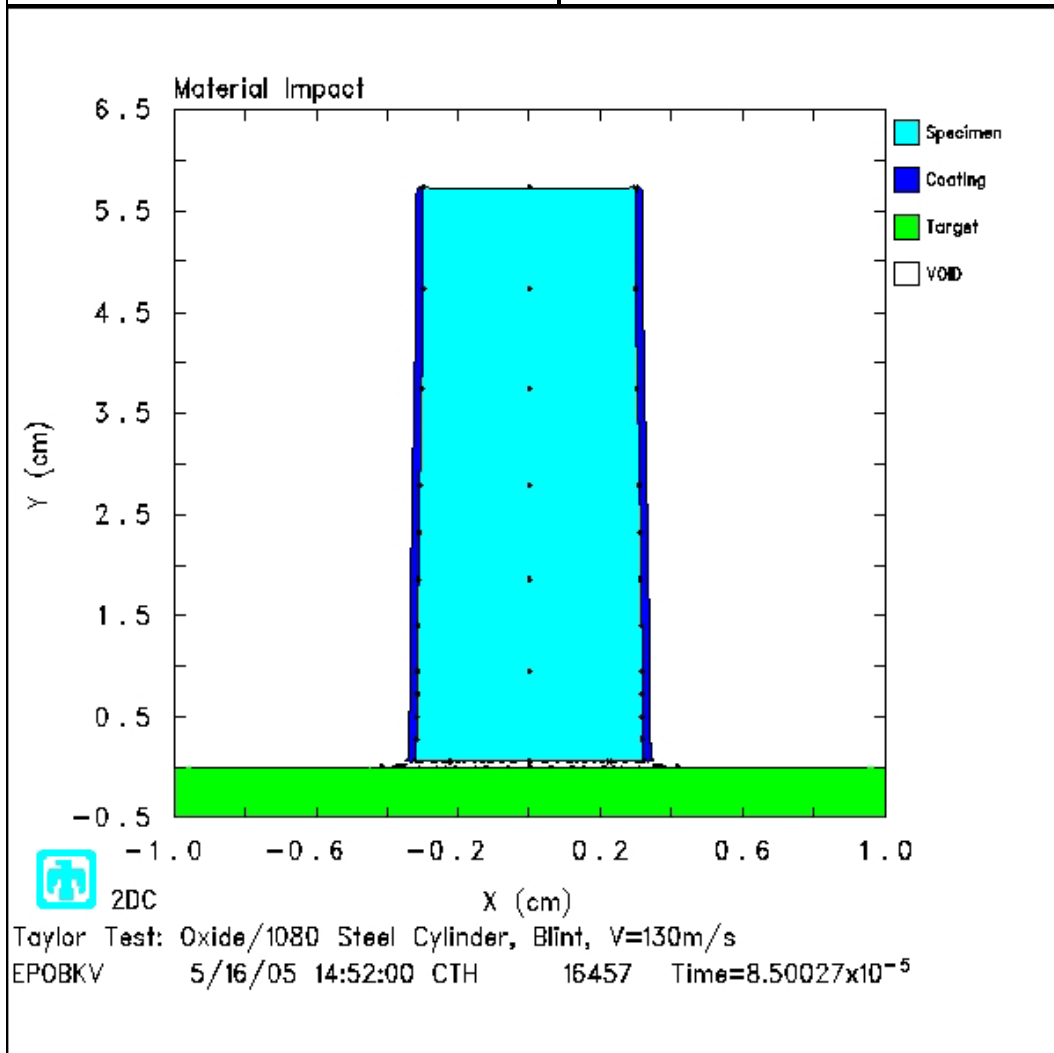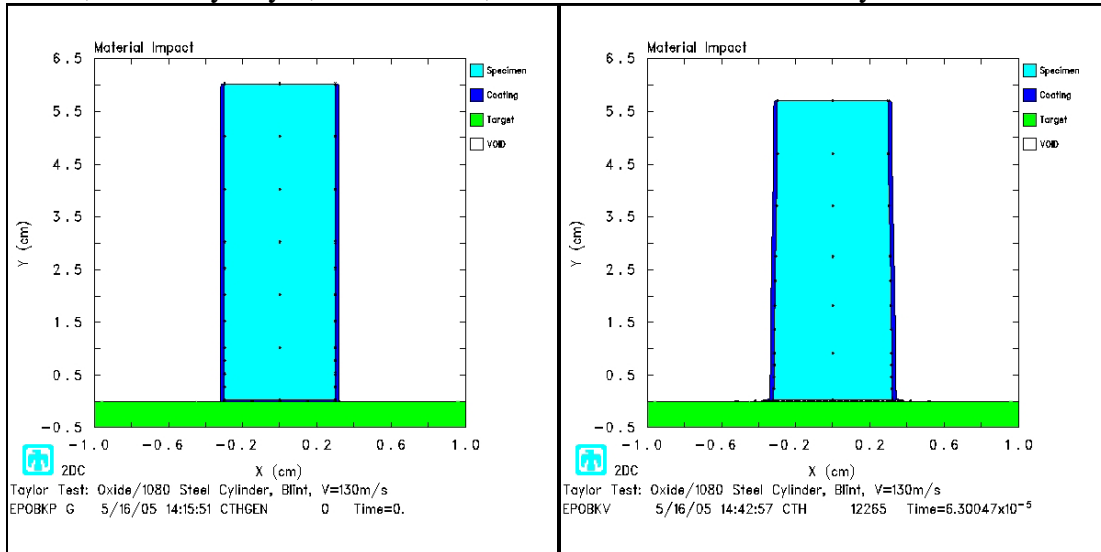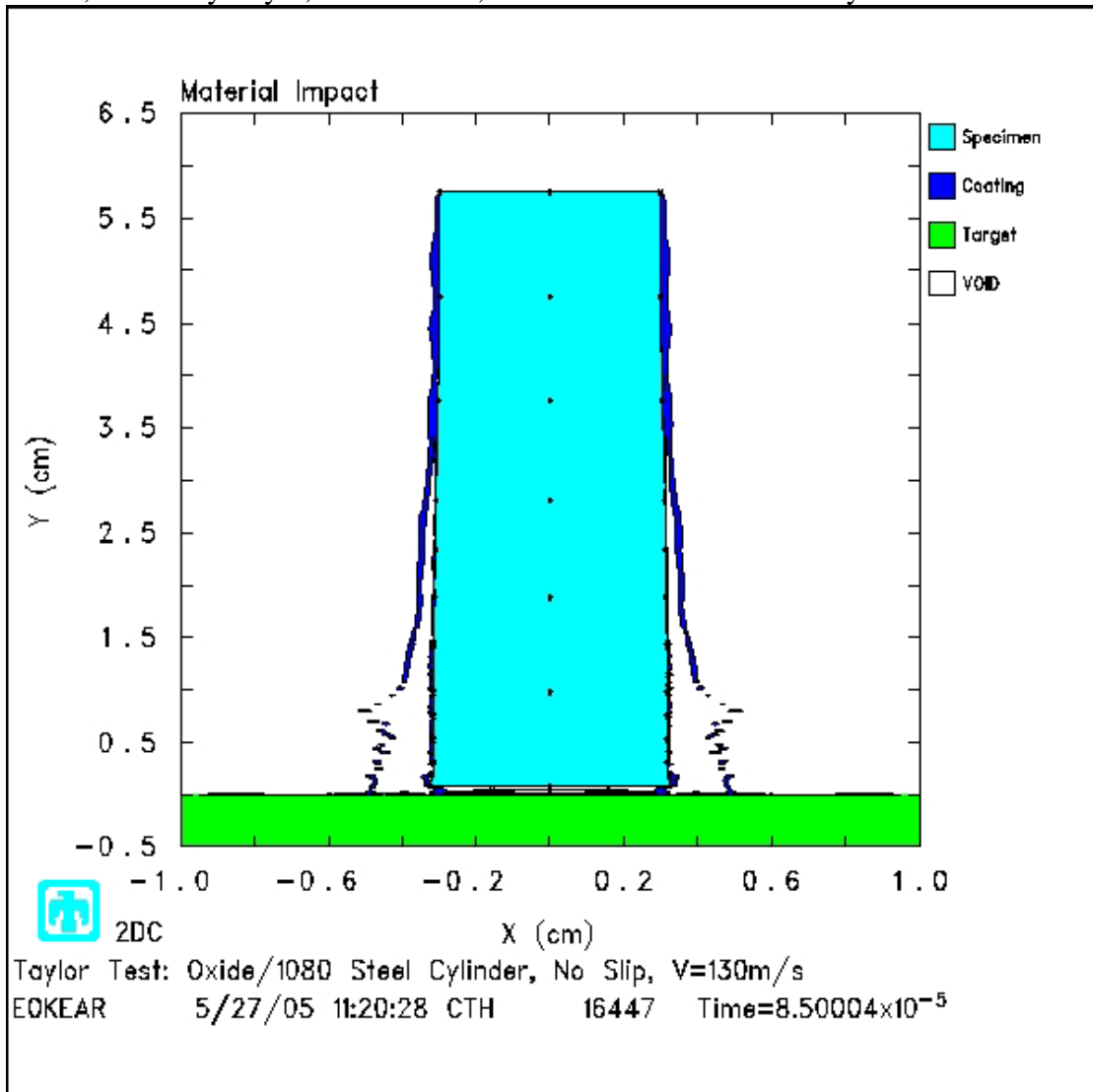
109
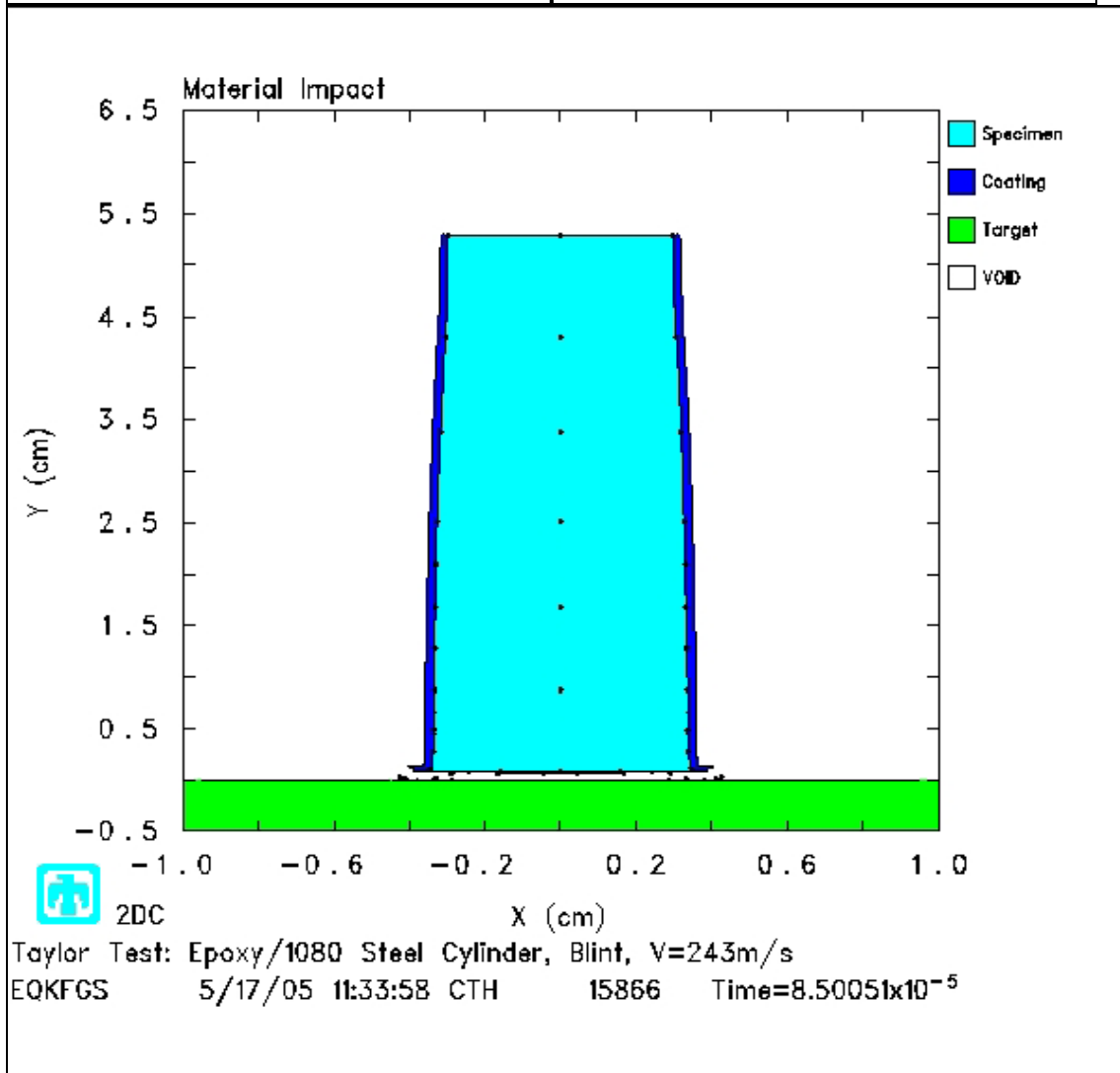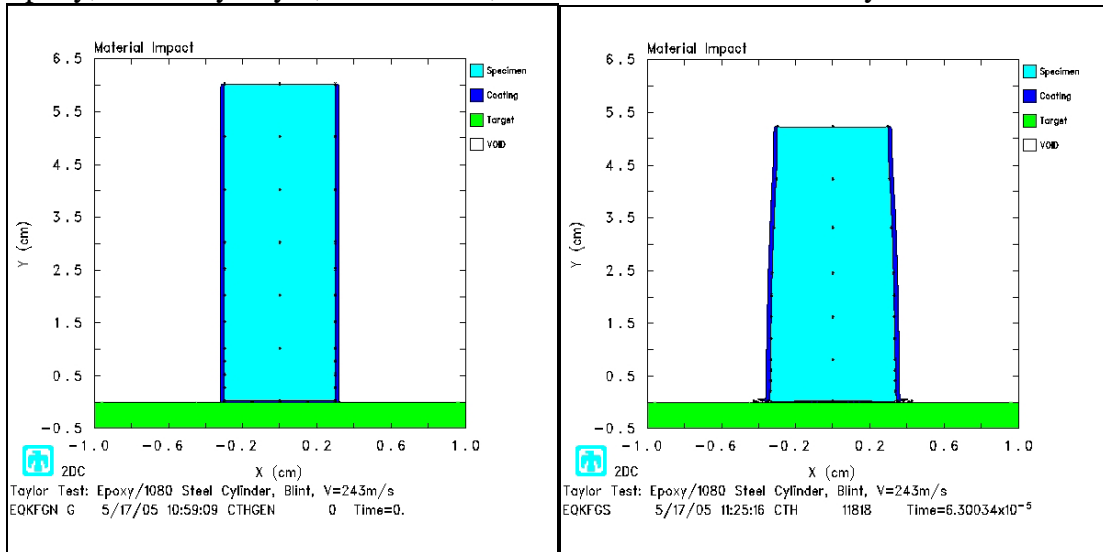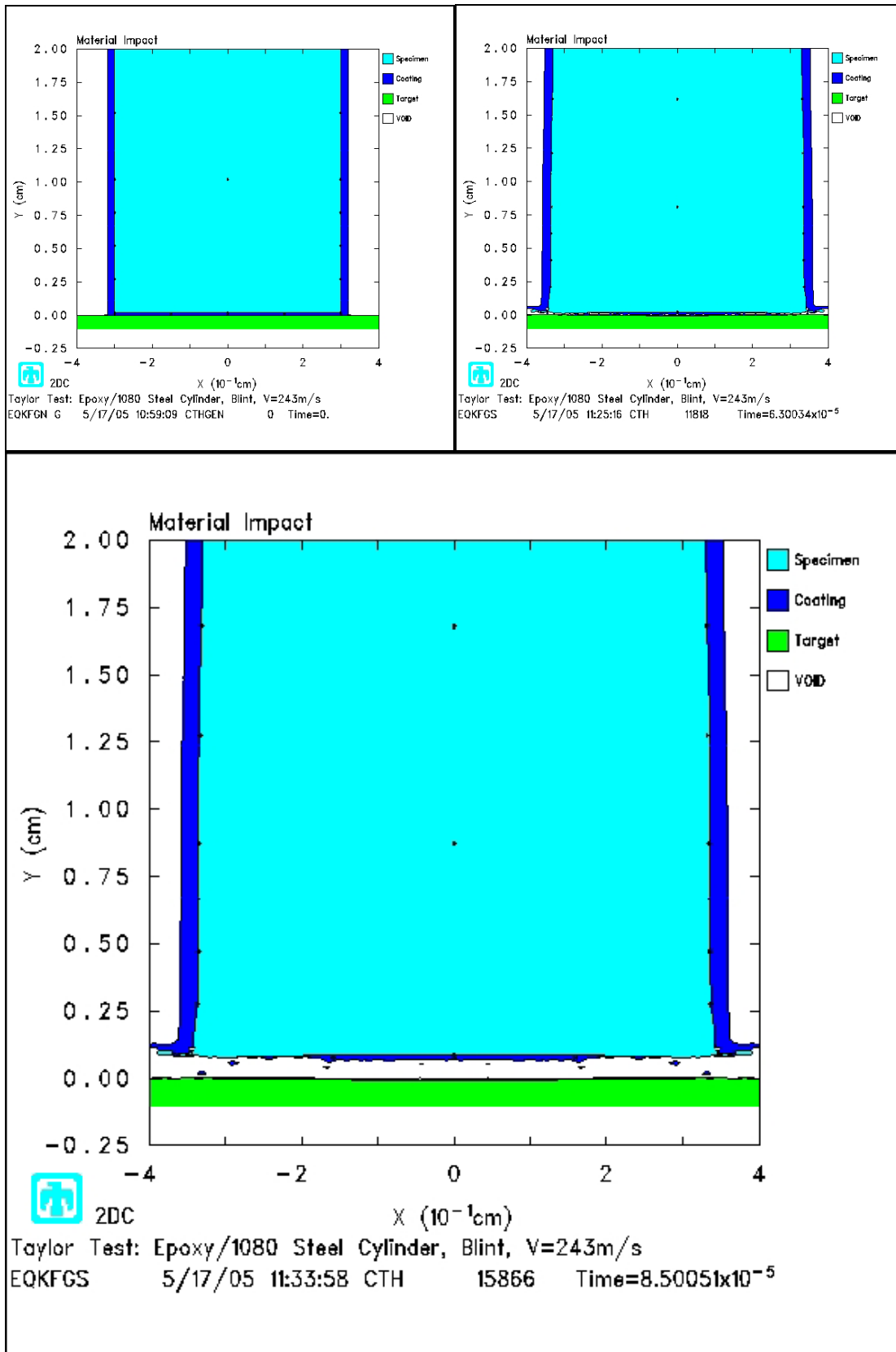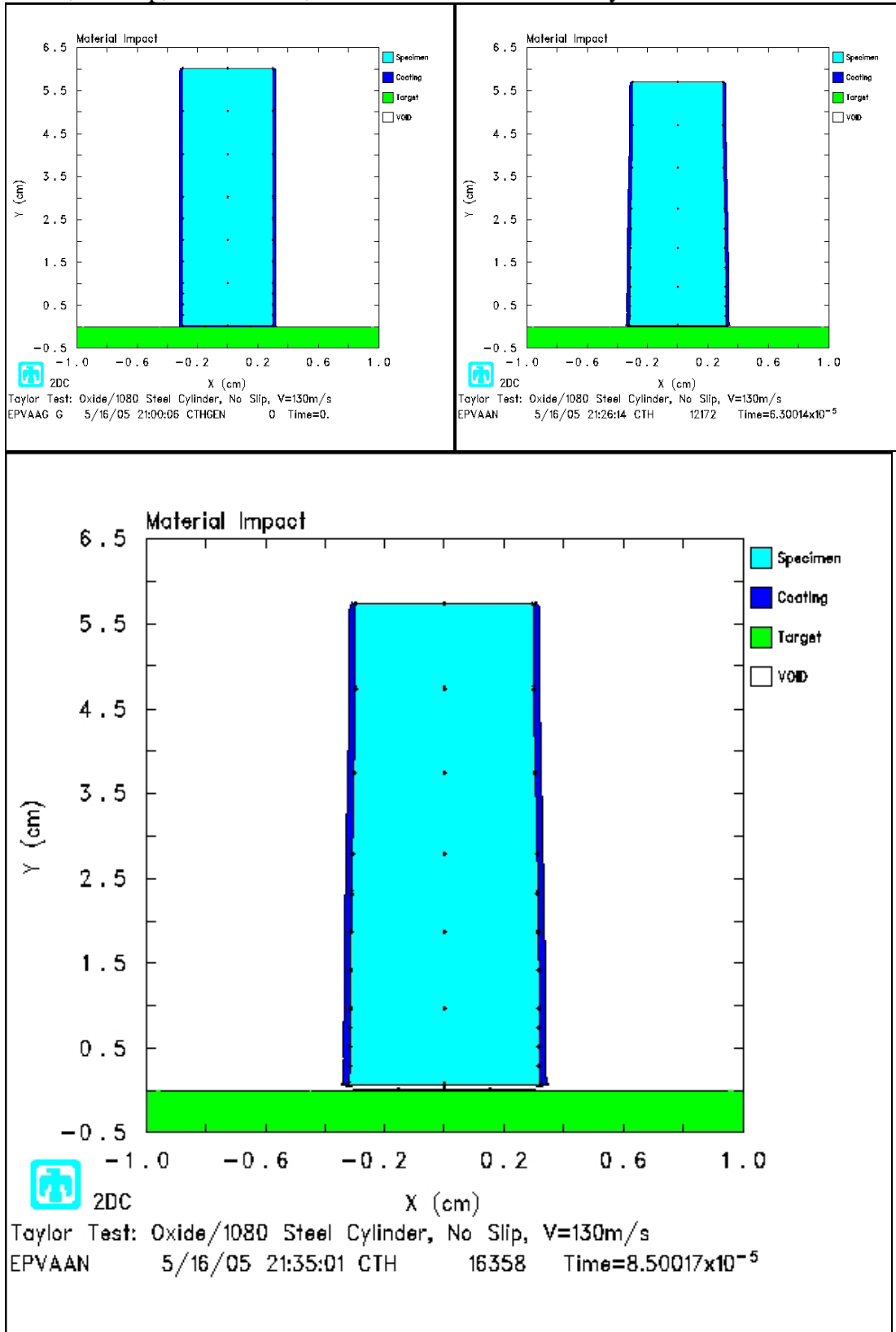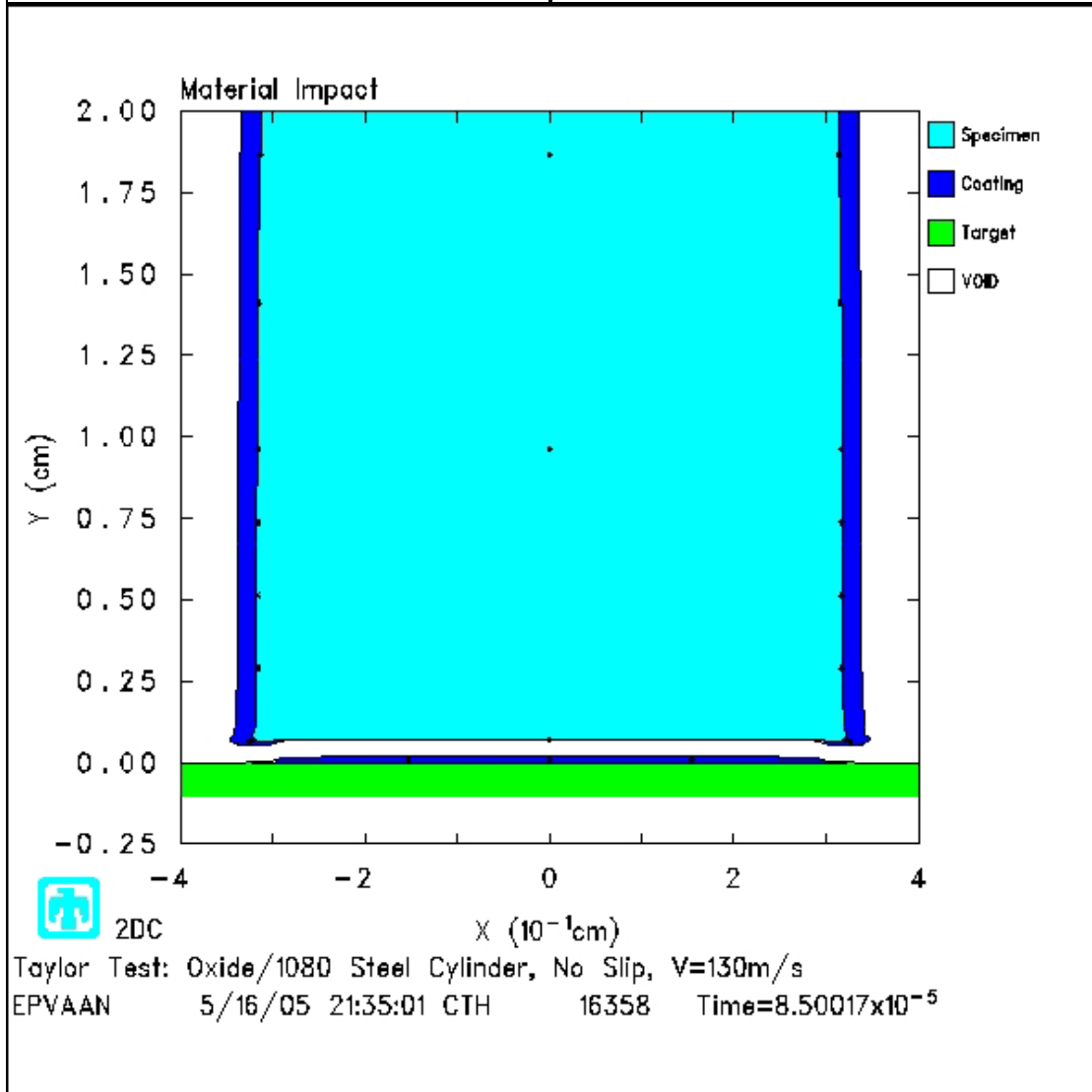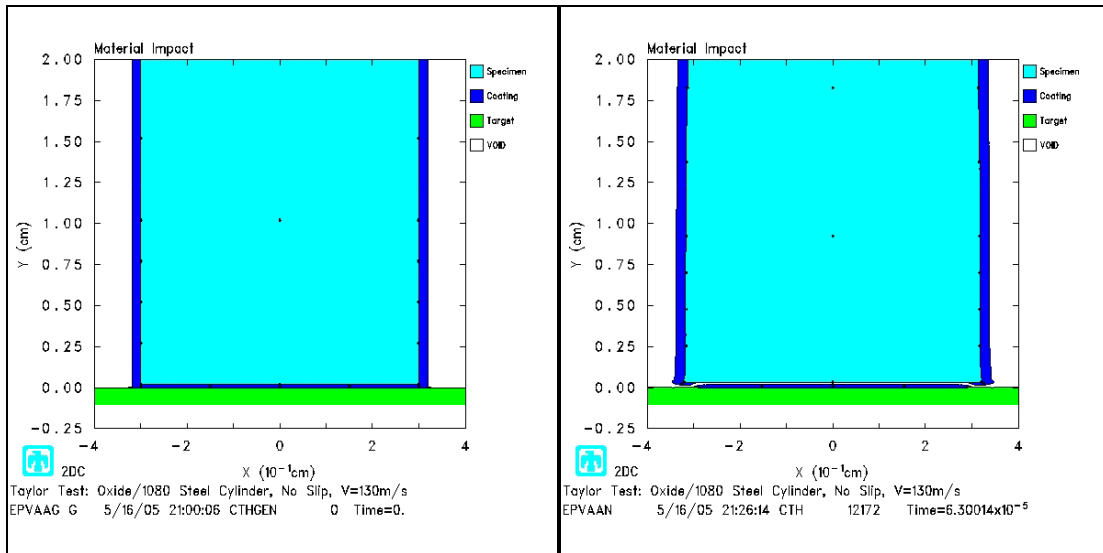
Oxide, Boundary Layer, V = 130 m/s, Fracture Pressure = 1.5e8 Dyne / cc
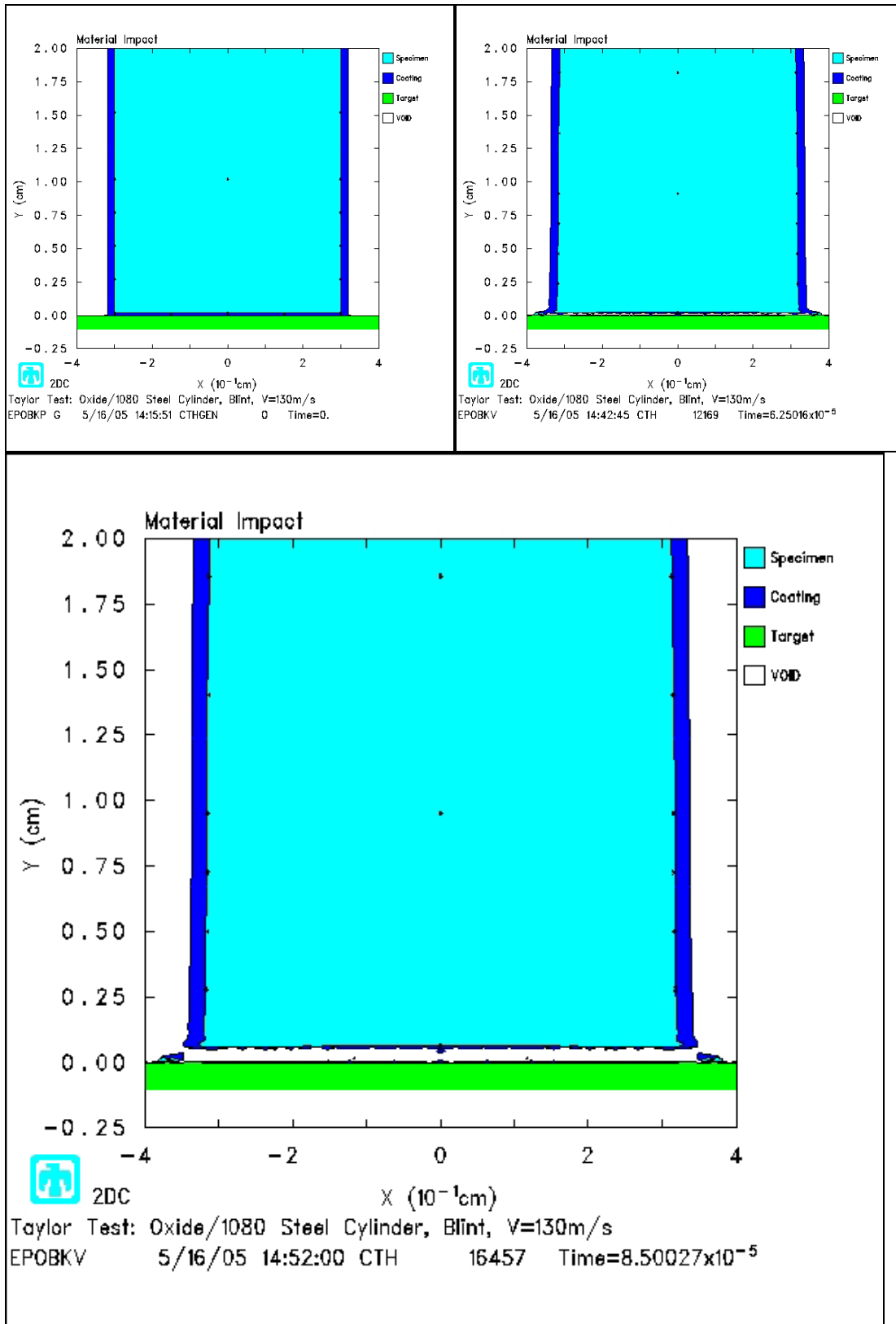
Oxide, Boundary Layer, V = 130 m/s, Fracture Pressure = 5.0e6 Dyne / cc

Appendix 5

Cost Comparison Tables

Variables		
Test Equipment Replacement Cost	$1,000,000.00	per failure
Uncoated Chipping Damage	175.00	ft / test
Completely New Coating every	4.00	tests

Common Information		
Workday	8.00	hr / day
1 section of rail	39.00	ft
Width of Coated Rail	9.50	in =
Track Length	52800.00	ft
Avg. Coating Thickness	0.02	cm
Uncoated test fails Once every	12	Tests
Cost of Rail	$1,000.00	per section
Replace	2	rail sections / failure
Total Coated Portion	35200	ft

New Rail Coating		Uncoated	Iron Oxide	Epoxy	Units
Initial Information					
	Portion Coated	17600	17600	17600	ft / coating
	Coating Effectiveness Factor	0.00%	23.00%	31.00%	reduced failure
Coating Application					
Materials	Coating Kit	$0.00	$33.32	$104.21	per gal
	Coating Kit	0	8	12	gal / 1000 ft
	Thinner	$0.00	$5.79	$14.21	per gal
	Thinner	0	5	15	gal / 1000 ft
Labor	Prep	0	2	2	man*hr / 1000 ft
	Apply	0	24	24	man*hr / 1000 ft
	Clean-Up	0	4	4	man*hr / 1000 ft
	Coater's Wages	$0.00	$19.00	$19.00	per man*hr
	Coating Application Cost	$0.00	$865.51	$2,033.67	per 1000 ft
	Coating Application Cost	$0.00	$0.87	$2.03	per ft of rail
	Coating Application Cost	$0.00	$3,808.24	$8,948.15	per test

Chipping Repair / Maintainence		Uncoated	Iron Oxide	Epoxy	Units
Amn't of Chipping Damage		175	134.75	120.75	ft / test
Material Removal Treatment					
Sand Blast	Mat'l	0	$1,920.00	$3,000.00	per 1000 ft
	Labor	0	$3,040.00	$5,168.00	per 1000 ft
	misc. Equip.	0	$115.00	$175.00	per 1000 ft
	Time	0	10	16	days / 1000 ft
	Sand Blast Cost	$0.00	$5,075.00	$8,343.00	per 1000 ft
	Sand Blast Cost	$0.00	$5.08	$8.34	per ft of rail
Water Blast	Mat'l	0	$0.00	$0.00	per 1000 ft
	Labor	0	$221.00	$578.00	per 1000 ft
	misc. Equip.	0	$0.00	$0.00	per 1000 ft
	Time	0	6.5	17	hr
	Water Blast Cost	$0.00	$221.00	$578.00	per 1000 ft
	Water Blast Cost	$0.00	$0.22	$0.58	per ft of rail

Material Re-Apply				
Material Coating	$0.00	$0.87	$2.03	per ft of rail
Labor Time	0.00	1.00	1.00	hr / 4 sq in
Re-Apply	$0.00	$541.50	$541.50	per ft of rail
Chipping Repair Cost				
Sand Blast	$0.00	$547.44	$551.88	per ft of rail
Water Blast	$0.00	$542.59	$544.11	per ft of rail
Sand Blast	$0.00	$36,883.80	$33,319.55	per test
Water Blast	$0.00	$36,556.77	$32,850.74	per test

Failure	Uncoated	Iron Oxide	Epoxy	Units
Rail Replacement				
Labor Workers	5	5	5	workers
Repair's Wages	$30.00	$30.00	$30.00	per hr
Install	5	5	5	days / failure
Alignment	10	10	10	days / failure
Labor Cost	$18,000.00	$18,000.00	$18,000.00	per failure
Material				
Coating Application Cost	$0.00	$0.87	$2.03	per ft of rail
Material Cost	$2,000.00	$2,067.51	$2,158.63	per failure
Avg. Rail Replacement Cost	$20,000.00	$20,067.51	$20,158.63	per failure
Cost of Failure	$0.00	$0.00	$58,659.12	per test

Cost Summary					
	Uncoated	Iron Oxide	Epoxy	Sum Total	Units
Sand Blast	$0.00	$40,692.05	$100,926.82	$141,618.87	per test
Water Blast	$0.00	$40,365.01	$100,458.01	$140,823.02	per test

Total Cost per Test			
Test Set-up cost	All Uncoated	All Iron Oxide	All Epoxy
$500,000.00	$43,333.33	$95,379.23	$102,448.95
$1,000,000.00	$85,000.00	$127,462.57	$131,198.95
$2,000,000.00	$168,333.33	$191,629.23	$188,698.95
$3,000,000.00	$251,666.67	$255,795.90	$246,198.95
$4,000,000.00	$335,000.00	$319,962.57	$303,698.95
$5,000,000.00	$418,333.33	$384,129.23	$361,198.95
$6,000,000.00	$501,666.67	$448,295.90	$418,698.95

Total Cost per Test			
Test Set-up cost	1/3 Each	2/3 Oxide	2/3 Epoxy
$500,000.00	$90,804.96	$91,570.99	$93,500.81
$1,000,000.00	$119,554.96	$123,654.32	$122,250.81
$2,000,000.00	$177,054.96	$187,820.99	$179,750.81
$3,000,000.00	$234,554.96	$251,987.66	$237,250.81
$4,000,000.00	$292,054.96	$316,154.32	$294,750.81
$5,000,000.00	$349,554.96	$380,320.99	$352,250.81
$6,000,000.00	$407,054.96	$444,487.66	$409,750.81

Cost of Completely Coated Track per Test vs. Payload Value

Cost of Sectionally Coated Track vs Payload Value

118

Bibliography

1. Rickerd, Gregory S. "An Investigation of a Simplified Gouging Model AFIT/GAE/ENY/05-M19". Master's Thesis, Air Force Institute of Technology, Wright-Patterson AFB OH, March 2005.

2. Szmerekovsky, Andrew G. The Physical Understanding of the use of Coatings to Mitigate Hypervelocity Gouging Considering Real Test Sled Dimensions AFIT/DS/ENY 04-06. PhD dissertation, Air Force Institute of Technology, Wright-Patterson AFB OH, September 2004.

3. Nicholas, Theodore and Rodney F. Recht. High Velocity Impact Dynamics, chapter 1 Introduction to Impact Phenomena, 1-63. New York NY: John Wiley and Sons., 1990.

4. Anderson, Charles G. "An Overview of the Theory of Hydrocodes," *International Journal of Impact Engineering*, 5:33-59 (1987).

5. Zukas, Jonas A. Introduction to Hydrocodes, San Diego CA: ELSEVIER Inc., 2004.

6. Cook, William H. "2D Axisymmetric Lagrangian Solver for Taylor Impact with Johnson-Cook Constitutive Model", Vol. 1. Air Force Research Lab, April 2000.

7. Nicholas, Theodore. "Tensile Testing of Materials as High Rates of Strain". Experimental Mechanics, 177-185, May 1981.

8. McGlaun, J.M., et al. "CTH: A three-dimensional Shock Wave Physics Code," *International Journal of Impact Engineering,* 10: 351-360 (1990).

9. Bell, R.L., et al., *CTH User's Manual and Input Instruction*. Albuquerque, NM: Sandia National Laboratories, 2003.

10. Palazotto, Dr; Cinnamon; Kennan; Blomer. "Development of a High Strain-Rate Constitutive Relationship for Hypervelocity Impact". Proceedings of the 2005 ASME International Congress, November 2005.

11. Furlow, Scott. Interview, Holloman AFB White Sands AFB, May 2005.

12. Hibbeler, R.C. *Mechanics of Materials*. Upper Saddle River, New Jersey: Prentice Hall, 2000.

13. Nguyen, Minh C. "Analysis of Computational Methods for the Treatment of Material Interfaces". Master's Thesis, Air Force Institute of Technology, Wright-Patterson AFB OH, March 2005.

14. Bowden & Freitag, "The Friction of solids at Very High Speeds". Proceedings of the Royal Society, Series A, 248 P 350-367, March 1958

15. Kennan, Zachary. "Determination of the Constitutive Equations for 1080 Steel and VascoMax300". Master's Thesis, Air Force Institute of Technology, Wright-Patterson AFB OH, June 2005.

16. Pantermuehl, P.J.; Smalley, A.J. "Friction Tests Typical Chock Materials and Cast Iron". Mechanical and Fluids Engineering Division Southwest Research Institute, 1997.

17. Hooser, Dr Michael. Interview, Holloman AFB White Sands AFB, December 2004.

1. REPORT DATE *(DD-MM-YYYY)* 13-06-2005	2. REPORT TYPE Master's Thesis	3. DATES COVERED *(From – To)* Aug 2004 – Jun 2005

4. TITLE AND SUBTITLE	5a. CONTRACT NUMBER
Cost Comparison of Existing Coatings for a Hypervelocity Test Rail	5b. GRANT NUMBER
	5c. PROGRAM ELEMENT NUMBER
6. AUTHOR(S) Blomer, Mark A., Ensign, USNR	5d. PROJECT NUMBER If funded, enter ENR #
	5e. TASK NUMBER
	5f. WORK UNIT NUMBER

7. PERFORMING ORGANIZATION NAMES(S) AND ADDRESS(S) Air Force Institute of Technology Graduate School of Engineering and Management (AFIT/EN) 2950 Hobson Way WPAFB OH 45433-8865	8. PERFORMING ORGANIZATION REPORT NUMBER AFIT/GAE/ENY/05-J01

9. SPONSORING/MONITORING AGENCY NAME(S) AND ADDRESS(ES) Dr. Neal Glassman, AFOSR (AFRL) 4015 Wilson Blvd, Room 713 Arlington, VA 22203-1954	10. SPONSOR/MONITOR'S ACRONYM(S)
	11. SPONSOR/MONITOR'S REPORT NUMBER(S)

12. DISTRIBUTION/AVAILABILITY STATEMENT

APPROVED FOR PUBLIC RELEASE; DISTRIBUTION UNLIMITED.

13. SUPPLEMENTARY NOTES

14. ABSTRACT

This study compared the relative costs, to the Department of Defense, of two different coatings used to protect a high speed test rail. Each coating was compared to the case of an uncoated rail with test conditions that caused catastrophic failure just after the test sled reached its maximum velocity. The total cost was finalize3d on a per test basis in order to sum cost of various expenditures that may only happen once every few tests.

To compare the protective properties of each coating, various coated and uncoated samples were tested via a cylinder specimen Taylor Impact Test. Each coating's protective properties, or coating effectiveness, were found by its radial deformation change at the impacted end of each cylinder relative to the uncoated cylinder. This deformation change, relative to the uncoated cylinder's deformation, is the coating's effectiveness.

Taylor Test results were then analyzed using the CTH hydrocode. CTH is able to model Taylor Impact Tests. CTH was used to understand the internal workings and results of the Taylor Tests in more depth. Verification between CTH and experimental Taylor Tests was done using final values for length, diameter and undeformed length of the cylinder.

15. SUBJECT TERMS

Impact, Impact Loads, Impact Tests, Shock Waves, Impact Shock

16. SECURITY CLASSIFICATION OF:			17. LIMITATION OF ABSTRACT	18. NUMBER OF PAGES	19a. NAME OF RESPONSIBLE PERSON Dr. A.N. Palazotto, USAF
a. REPORT	b. ABSTRACT	c. THIS PAGE	UU	134	19b. TELEPHONE NUMBER *(Include area code)* (937) 255-3636 x4599 (anthony.palazotto@afit.edu)
U	U	U			